Fakultät für Medizin

TRPC6 as a novel treatment target in vascular remodeling: in vitro and in vivo analyses

Ganildo Cepele

Vollständiger Abdruck der von der Fakultät für Medizin der Technischen Universität München zur Erlangung des akademischen Grades eines Doktors der Medizin (Dr. med.) genehmigten Dissertation.

Vorsitz: apl. Prof. Dr. Bernhard Haslinger

Prüfer*innen der Dissertation:

1. Prof. Dr. Heribert Schunkert
2. apl. Prof. Dr. Christian Kupatt-Jeremias

Die Dissertation wurde am 02.08.2022 bei der Technischen Universität München eingereicht und durch die Fakultät für Medizin am 21.02.2023 angenommen.

Acknowledgment

I would like to express my gratitude to my primary supervisor, Prof. Dr. Heribert Schunkert, whose expertise was invaluable in formulating the research questions and methodology. I wish to show my appreciation to Prof. Dr. Adnan Kastrati for being my second advisor and for guiding me throughout this project. I would also wish to express my deepest gratitude to my tutor, Dr. Thorsten Kessler, for the insightful feedback and continuous support, which brought my work to a higher level. I would also wish to thank Jana Wobst, Tan An Dang and Carina Mauersberger whose assistance was a milestone in the completion of this project.

Table of Contents

List of Abbreviations vii
List of Figures x
List of Tables xi

1 Introduction 1

1.1 Coronary artery disease: Epidemiology and risk factors 1
1.1.1 Molecular and cellular mechanism in atherosclerosis 2
1.1.2 Therapeutic options 4
1.1.3 Vascular remodeling and restenosis after PCI 5
1.2 Identification of novel targets in vascular injury 7
1.2.1 Unbiased proteome-wide analysis of vascular injury 8
1.2.2 TRPC6 9
1.3 Aim of this study 13

2 Material 15

2.1 Chemicals 15
2.2 Buffers, media and solutions 18
2.3 Cell lines 20
2.4 Antibodies 21
2.4.1 Primary antibodies 21
2.4.2 HRP-conjugated secondary antibodies 21
2.5 Mice 21
2.6 Compounds used 22
2.7 Commercially available kits 22
2.8 Devices and utensils 23
2.9 Software 25

3 Methods 27

3.1 Animal experiments 27
3.2 Immunoblotting 28
3.2.1 Protein isolation from femoral arteries 28
3.2.2 Protein quantification 28

3.2.3 Western Blots 29
3.3 Cell culture 30
3.4 VSMC migration assays 32
3.4.1 Scratch wound healing assay 32
3.4.2 Migration radius assay 32
3.5 VSMC proliferation assays 33
3.6 Histological analysis 34
3.6.1 Sectioning 34
3.6.2 Staining 34
3.6.3 Microscopy 35
3.6.4 Quantification of neointima formation 35
3.7 Binary restenosis analysis 36
3.8 Statistical analysis 37

4 Results 39

4.1 Validation of increased Trpc6 expression 39
4.2 TRPC6 and VSMC migration 40
4.2.1 Scratch wound assay 40
4.2.2 Radius migration assay 40
4.3 TRPC6 and VSMC proliferation 40
4.4 Neointima formation in mice lacking Trpc6 41
4.5 *TRPC6* expression and restenosis 43

5 Discussion 49

6 Summary 55

7 Bibliography 57

List of Abbreviations

°C	degree Celsius
ACS	acute coronary syndrome
ACC	American College of Cardiology
AHA	American Heart Association
Ank	Ankyrin
BCA	Bicinchoninic acid
BME	ß- mercaptoethanol
BMI	body mass index
BMS	bare metal stent
CABG	coronary artery bypass grafts surgery
CAD	Coronary artery disease
cc	coiled-coin
CHD	Coronary heart disease
Chr	chromosome
CIRB	IP3 receptor-binding region
cMMb	recombination rate (cM per MB)
CVD	Cardiovascular disease
DAG	diacylglycerol
DAPT	dual antiplatelet treatment
DES	drug-eluting stent
EC	endothelial cells
ECM	extracellular matrix
EEL	external elastic lamina
EER	early elastic recoil
e.g.	exempli gratia
ER	endoplasmatic reticulum
FSGS	focal segmental glomerular sclerosis
GAPDH	Glyceraldehyde 3-phosphate dehydrogenase
GO	gene ontology
GTEx	Genotype-Tissue Expression project
GWAS	genome-wide association studies

h	hours
HF	heart failure
i.e.	id est
IEL	internal elastic lamina
IL	interleukins
IP_3	inositol-1,4,5-trisphosphate (IP3)
ISR	in stent-restenosis
LC	liquid-chromatography
LC-MS	liquid chromatography mass spectrometry
LDL	low-density lipoprotein
LIMA	left internal mammary artery
Mb	millions of base pairs
MI	myocardial infarction
MMP	matrix metalloproteinase
min	minute
MS	mass spectrometry
MS/MS	tandem mass spectrometry
mTOR	mammalian target of rapamycin
OAG	1-Oleoyl-2-acetyl-sn-glycerol
OLR1	oxidized LDL-receptor 1
oxLDL	oxidized low-density lipoprotein
PBS	phosphate buffered saline
PCI	percutaneous coronary intervention
PDGF	platelet-derived growth factor
PI3K	phosphatidylinositol-3-kinase
PLC	Phospholipase C
PTCA	percutaneous transluminal coronary angioplasty
$PI(4,5)P_2$	phosphatidylinositol-4,5-bisphosphate
RIPA	radioimmunoprecipitation
ROC	receptor operated calcium current/channel
SDS	sodium dodecyl sulfate
sec	seconds
SMC	smooth muscle cells
SNP	single nucleotides polymorphism

STEMI	ST-elevating myocardial infarction
(N) STEMI	(Non-)ST-elevating myocardial infarction
TF	tissue factor
TGF-ß	transforming growth factor ß
TRP	transient receptor potential
TRPC6	canonical transient receptor potential channel 6
$TRPC6^{-/-}$	TRPC6-deficient mice
US	United States
VSMC	vascular smooth muscle cells
wt	wild type
α_1-AR-NSCC	α-1-adrenoreceptor-activated nonselective cation channels

List of Figures

Figure 1 Atherosclerotic lesions development. 2
Figure 2 TRP channel structure 10
Figure 3 TRPC as receptor operated calcium current (ROC) 11
Figure 4 Representative Western Blot showing the expression level of TRPC6 in non-injured femoral arteries (NI) and injured femoral arteries 39
Figure 5 TRPC6 as a novel treatment target in vascular remodeling 41
Figure 6 Neointima formation in Trpc6$^{-/-}$ mice 42
Figure 7 Angiographic follow-up analysis and the risk of restenosis after coronary stenting 46
Figure 8 TRPC6 inhibition as a complementary pathway to reduce neointima formation . 53

List of Tables

Table 1 List of chemicals used 15
Table 2 Commercially available cell line 20
Table 3 HRP-conjugated secondary antibodies used 21
Table 4 List of used compounds 22
Table 5 List of commercially available kits 22
Table 6 List of used devices and utensils 23
Table 7 List of software used 25
Table 8 Cell number seeded 31
Table 9 Baseline and procedural characteristics of individuals with available rs2513192 genotype 44
Table 10 Multivariate analysis of rs2513192 AA genotype with in-stent restenosis after PCI with stent implantation 47

1 Introduction

1.1 Coronary artery disease: Epidemiology and risk factors

According to the World Health Organization, cardiovascular diseases (CVD) are the leading causes of death in the last 15 years, being responsible for the death of around 17.9 million people in 2019 (World Health Organization; 2021). Within the large group of CVD, coronary artery disease (CAD) and its sequelae were responsible for 43.8 % of all deaths in the United States (US) in 2015, followed by stroke with 16.8 %, and high blood pressure by approximately 10 % (Benjamin et al., 2018). The calculated lifetime risk for CAD at the age of 40 is approximately 50 % for men and 32 % for women (Lloyd-Jones et al., 1999). CAD is the result of decreased perfusion of the heart muscle, which can lead to different and life-threatening complications, such as myocardial infarction (MI) or ischemic heart failure (HF). The burden of CVD is believed to increase, with approximately 41 % of the US population being affected by some form of CVD by 2030 (Heidenreich et al., 2011). As a complex and multifactorial disease, CAD can be influenced by modifiable environmental factors and genetic susceptibility (Kessler et al., 2013). Different risk factors such as smoking, abnormal lipids, diabetes, psychosocial factors, abdominal obesity and hypertension are summed up under the term ‘modifiable risk factors’, as they can be treated with lifestyle changes and therapeutic interventions (Yusuf et al., 2004). A positive family history is known to be another relevant risk factor. The heritability of CAD and its underlying genetic mechanism remained unknown for decades [for an overview see (Mayer et al., 2007)] before genome-wide association studies (GWAS) of CAD and MI were introduced [for an overview see (Kessler et al., 2016)]. However, one of the main mechanisms leading to CAD is atherosclerosis, an inflammatory vascular disease, which over decades leads to plaque formation in the inner lining of the coronary arteries and obstruction of blood flow (Libby et al., 2011).

1.1.1 Molecular and cellular mechanism in atherosclerosis

Atherosclerosis is nowadays known as a chronic inflammatory disease within the arterial wall, leading to formation of atherosclerotic plaques (Tedgui & Mallat, 2006; Weber et al., 2008). The arterial wall consists of three structurally different layers: the innermost Tunica intima, the middle Tunica media and the outermost Tunica adventitia (Rhodin, 1980) (**Figure 1a**). An external elastic lamina (EEL) separates the tunica adventitia from the tunica media. The Tunica intima consists of resident smooth muscle cells (SMC) and a layer of endothelial cells (EC), which line the internal surface of blood vessels and overlie a basement membrane (Libby et al., 2011). An internal elastic lamina (IEL) lines the EC layer on its abluminal site and separates the tunica intima from the tunica media (Lee et al., 2005).

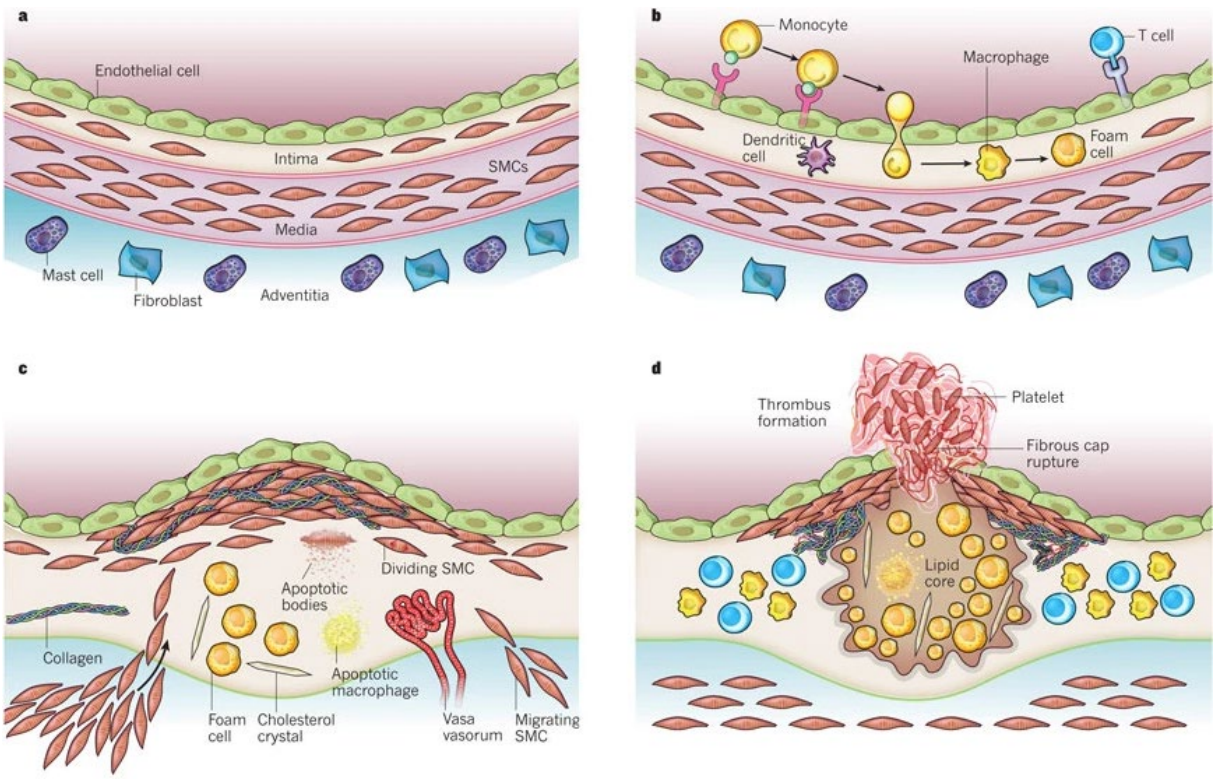

Figure 1: Atherosclerotic lesions development. Reprinted by permission from Macmillan Publishers Ltd: Figure 1 from Nature 2011. 473(7347):317-325 (Libby et al. 2011), copyright © 2011.

"Response to injury" hypothesis is a widely accepted hypothesis of coronary atherosclerosis development, which is initiated by endothelial dysfunction due to inflammatory processes and high blood low-density lipoprotein (LDL)-levels, followed by accumulation of lipids and macrophages into the intima and resulting in plaque formation

(Ross, 1993). The endothelium plays under normal conditions a key role in maintaining a physiological hemostasis by regulating different processes such as inflammation, platelet aggregation, thrombosis and SMC proliferation (Schwartz et al., 2010). Alterations in the monolayer of EC, when subjected to irritative stimuli (dyslipidemia, hypertension or pro-inflammatory mediators), promote an up-regulation of adhesion molecules and an increased cell permeability (Hansson, 2005; Libby et al., 2010; Libby et al., 2011). The increased endothelial cell permeability and extracellular matrix (ECM) alteration in the intima promote the infiltration and retention of cholesterol-laden LDL-particles into the artery wall (Libby et al., 2011). LDL is oxidized in the intima, which leads again to endothelial activation with increased expression of adhesion molecules and pro-inflammatory genes (**Figure 1b**). That triggers the adhesion of blood cells, more likely monocytes and lymphocytes, to the artery wall (Hansson, 2005; Lusis, 2000). Once in the intima, monocytes differentiate into macrophages and engulf oxidized LDL-particles (oxLDL) and ultimately, the cell turns into a foam cell (**Figure 1b**). Not only macrophages, but also other immune cells, like B- and T-lymphocytes, dendritic cells and mast cells accumulate and contribute to plaque formation by expressing pro-inflammatory cytokines and growth factors, which also drive the proliferation and migration of SMC from the tunica media into the tunica intima (**Figure 1c**) (Hansson, 2005; Libby et al., 2011). In the intima, a fibrous cap is formed due to the production by SMC of ECM molecules, collagen, elastin, proteoglycans and glycosaminoglycans (Libby et al., 2019). The enlargement of plaque over time causes a luminal narrowing and an impaired arterial perfusion under increased oxygen demand, which is clinically presented by producing angina pectoris or ischemia symptoms such as fatigue, dyspnoea and exercise intolerance (Libby et al., 2019). Plaques may not cause any problem and remain silent for decades. Activated macrophages, mast cells and T-cells produce different molecules and proteases that can degrade the fibrous cap of the plaque (**Figure 1d**) (Libby et al., 2010). They can also provoke the death of SMC, one of the most important interstitial sources of collagen for the blood vessels (Libby, 2009). The disruption of plaque exposes prothrombotic material to the bloodstream, triggering sudden blood flow obstruction of an artery and resulting e.g., in an acute coronary syndrome (ACS) or stroke (Libby et al., 2010). In coronary arteries, atherosclerosis might be clinically presented as an acute event (ACS) or chronic event (stable angina – now termed chronic coronary syndrome). Most of other complications such as ischemic cardiomyopathy, peripheral arterial disease, HF and arrhythmias arise as a consequence of atherosclerosis (Dzau et al., 2006; Libby et al., 2019).

1.1.2 Therapeutic options

The aim of CAD and atherosclerosis management is to reduce patients' symptoms, prevent plaque rupture and improve prognosis (Knuuti et al., 2019). Lifestyle modification by managing risk factors and implementation of healthy behaviors leads to a decreased number of cardiovascular events (Knuuti et al., 2019). They provide additional benefit over the medical therapy or revascularization procedures. However, progression of atherosclerosis increases patients' symptoms and reduces their quality of life. Revascularization is the gold standard in symptomatic coronary disease and lesions after ischemia, aiming to restore adequate blood flow to undersupplied myocardial territories due to severe coronary obstruction or occlusion (Neumann et al., 2018). Revascularization encompasses different techniques such as percutaneous coronary intervention (PCI) or also known as percutaneous transluminal coronary angioplasty (PTCA) and coronary artery bypass grafts surgery (CABG) (Byrne et al., 2017). CABG is the preferred method in stable complex obstructive CAD (Byrne et al., 2017). Advances made in CABG procedure such as the usage of the off-pump technique, the usage of left internal mammary artery (LIMA) and avoidance of saphenous vein as graft, avoidance of sternotomy by performing a lateral thoracotomy and improvements of postoperative pharmacotherapy contributed to the success of CABG in prolonging life and reducing symptoms (Cohn, 2010; Deb et al., 2013). However, PCI has become the most frequently revascularization approach performed nowadays (Byrne et al., 2017). PCI is the preferred reperfusion technique in stable CAD with limited complexity and in the emergency situations, like e.g. ACS (Neumann et al., 2018). Compared with CABG, patients who underwent PCI had a more rapid recovery and a better quality of life at one month time point (Kulik, 2017). During a PCI procedure, a wire-guided catheter with a tiny balloon on its tip is inserted via femoral or radial artery under local anesthesia and threaded through the arteries until it reaches the narrowed area in the coronary arteries. The balloon is then inflated to widen the narrowed area and restore the blood flow. The increased arterial lumen size is achieved by stretching the media and adventitia (Byrne et al., 2017; Grüntzig, 1978). Two main complications associated with balloon angioplasty brought the need of PCI evolution: 1) high rate of immediate emergency revascularization due to vessel reclosure and 2) high rate of restenosis (Byrne et al., 2017). To overcome these complications, nowadays stents are placed. A stent eliminates the vessel recoil and helps to keep the lumen opened after the balloon is deflated and removed (Byrne et al., 2017). While different stent types have enormously improved patients' clinical outcome, restenosis and late stent thrombosis still remain serious concerns for physicians. After stent placement, a dual antiplatelet

treatment (DAPT) with aspirin and a $P2Y_{12}$ inhibitor is recommended, with a different DAPT duration depending on different factors such as stent type and clinical presentation (Neumann et al., 2018). A lifetime-long intake of aspirin should follow (Neumann et al., 2018).

1.1.3 Vascular remodeling and restenosis after PCI

PCI is a widely used method worldwide for treating single or multivessel obstructive CAD, with more than two million interventions performed each year. However, PCI is associated with an increased need of repeated revascularization due to restenosis compared to CABG (Serruys et al., 2009). Restenosis can be detected either clinically or by angiographic follow-ups (Jukema et al., 2012). Recurrent angina or ischemia-related symptoms requiring reintervention characterize clinical restenosis (Cutlip et al., 2007), while a vessel's lumen diameter reduction of more than 50 % either with or without stent implantation is angiographically defined as restenosis (Buccheri et al., 2016; Cutlip et al., 2007). By analyzing angiographic follow-up data of more than 10,000 patients, Cassese et al showed that restenosis after PCI was associated with a higher mortality at a four-year time point, even in asymptomatic patients (Cassese et al., 2014).

Restenosis occurs as an excessive reaction of the vessel wall to injury. It includes three different important mechanisms: (I) early elastic recoil (EER), (II) vascular remodeling, (III) neointimal hyperplasia (Buccheri et al., 2016). EER is one of the first responses after vascular injury, caused by balloon overstretch of the elastic fibers of IEL and EEL and resulting in a lumen loss of up to 40 % (Buccheri et al., 2016). Vascular remodeling is defined as a functional and structural change beneath the arterial wall (specially media and adventitia) in response to injury, as a physiological healing response allowing adaption and repair (Galis & Khatri, 2002). The neointimal hyperplasia is a reparative process at the site of injury in case of stent placement (Kim & Dean, 2011), characterized mainly by migration and proliferation of SMC, the accumulation of inflammatory cells and ECM deposition (Newby & Zaltsman, 2000). Platelet adhesion and aggregation to the endothelial wall is triggered by endothelial denudation after mechanical vascular injury, whereby tissue factor (TF) is released into the bloodstream and an inflammatory response is initiated. TF activates the coagulation cascade, that leads to thrombus formation (Mitra et al., 2006). Through further platelet

and leukocyte activation, different growth factors such as platelet-derived-growth factors (PDGF), transforming growth factor ß (TGF-ß) and proinflammatory cytokines such as interleukins (IL) IL-1, IL-6, IL-8 are released. They act as a chemoattractant to the phenotypically modified SMC (Lee et al., 2004). Physiologically, vascular smooth muscle cells (VSMC) in the tunica media of mature blood vessels are quiescent, stable cells and have a differentiated contractile phenotype (Mitra et al., 2006). However, in response to injury, they might turn into a synthetic phenotype by increasing their ECM synthesis as well as their migration and proliferation capacity. This process is also known as VSMC phenotype modulation [reviewed in (Rensen et al., 2007)].

Changes in ECM´s composition have been associated with pathological conditions in atherosclerosis or restenosis (Chistiakov et al., 2013; Frangogiannis, 2017). Histopathological samples of coronary arterial in-stent restenotic tissue have shown an increased accumulation of ECM contributing to intimal hyperplasia in in stent-restenosis (Chung et al., 2002). The ECM is a non-cellular three-dimensional structure, which provides mechanical support to all tissues with a different composition for every organ. Besides its structural support, ECM plays an important role in influencing cell behavior by regulating cell migration, proliferation, adhesion, apoptosis and differentiation. It is composed of different proteins like collagen, proteoglycans and glycoproteins (Bonnans et al., 2014; Chistiakov et al., 2013). A key role in the pathogenesis of restenosis play the matrix metalloproteinases (MMP) i.e. enzymes, which are able to degrade ECM components (Galis & Khatri, 2002). An increased expression of MMP in the rat carotid artery after balloon angioplasty was shown to be associated with an increased migration and neointimal lesion (Bendeck et al., 1994). Furthermore, MMP inhibition was found to reduce SMC migration *in vivo* (Forough et al., 1996).

To overcome the plain old balloon angioplasty (POBA) limitations, stents were placed in the artery wall (Byrne et al., 2017). By preventing the EER and constrictive remodeling, the restenosis rate dropped to 17 – 41 % compared to 32 – 55 % in the pre-stent era (Buccheri et al., 2016). A thinner stent strut in BMS was shown to significantly reduce the rate of restenosis (Kastrati et al., 2001). However, neointima formation and the need for repeated revascularization raised many concerns regarding BMS safety compared to CABG (Serruys et al., 2009; Stefanini & Holmes, 2013). The introduction of drug-eluting stents (DES), which locally release antiproliferative agents, reduced the need of revascularization compared to BMS and further dropped the early in stent-restenosis (ISR) rate to < 10 % (Moses et al., 2003; Stefanini & Holmes, 2013).

However, an increased incidence of late stent thrombosis compared to BMS (Lüscher et al., 2007) possibly caused by impaired re-endothelialization and delayed arterial healing raised initial concerns regarding their safety (Joner et al., 2006). A prolonged DAPT is therefore indispensable, but at the cost of an increased risk of bleeding and death (Cassese et al., 2015). Human coronary autopsy stents revealed that neoatherosclerotic lesions occur earlier and with a higher incidence in DES compared to BMS (31 % vs. 16 %, $p< 0.001$) (Nakazawa et al., 2011). During neoatherosclerosis, it comes to a faster development of atherosclerotic plaques compared to atherosclerosis due to the incomplete regeneration of the endothelium and the higher uptake of circulating lipids in the intima (Nakazawa et al., 2011). The development of novel stent technologies remains nowadays the most promising target to reduce restenosis and neointima formation.

1.2 Identification of novel targets in vascular injury

A huge progress has been made in the last decades in identifying the genomic of mankind. Genetic profiling analysis is important in understanding human evolution, the causation of the disease and the interaction between heredity and environment in defining the human condition. Venter et al identified approximately 30,000 genes, responsible for encoding more than one million proteins (Venter et al., 2001). Proteins play a key role within a living cell in maintaining homeostasis. They carry out the major part of the cellular function and are responsible for the phenotype of the cells (Graves & Haystead, 2002). All expressed proteins produced by a tissue under physiological or pathological conditions at a particular time is defined as proteome (Deracinois et al., 2013). The term ‘proteome’ was first used by Wilkins et al in 1996 to define it as “PROTein complement expressed by a genOME” (Wilkins et al., 1996). The systematic analysis of proteins to identify their structure, function, quantity, expression and modification is also known as ‘proteomics’ (Peng & Gygi, 2001). The proteome, compared to the cell static genome, is dynamic and complex by regulating from time to time its gene expression depending on external stimuli and cell to cell interaction (Aslam et al., 2017; Peng & Gygi, 2001). Differential display proteomics is a fundamental approach in proteomics for studying pathogenesis in a wide range of diseases and comparing protein levels, with the objective of identifying proteins that are up - or downregulated in a disease specific manner (Pandey & Mann, 2000). For that reason,

knockout mice models can be used to identify potential target proteins that are differentially expressed in presence or absence of a protein of interest (Lee et al., 2012). The comparison of the quantitative proteome expression under different conditions can be assessed by liquid-chromatography- mass spectrometry (LC-MS) (Shen et al., 2014). There are three basic technological concepts where proteomics analysis is based: 1) a method to fractionate complex protein or peptide mixtures 2) MS to acquire necessary data and identify individual proteins 3) bioinformatics to analyze the acquired data (Yu et al., 2010). The analysis of proteins or peptides by MS can be divided in two categories: a) peptide mass analysis, where a mass spectrum is created by measuring all the individual peptides in a mixture and b) amino acid sequencing, which is used to fragment the peptides into smaller peptides and deducing the amino acid sequence by using a procedure known as tandem mass spectrometry (MS/MS) (Graves & Haystead, 2002). In the analysis of large raw amounts of data generated by MS-based proteomics, the fragmented protein sequences are assigned to a certain fragment ion spectra, using different computational software tools (Nesvizhskii et al., 2007).

1.2.1 Unbiased proteome-wide analysis of vascular injury

The physical injury of the arterial wall during a PCI procedure causes an increased intimal thickness of the internal side of the lesion or also known as sub-endothelial scars (Clowes et al., 1983; Newby & Zaltsman, 2000). Different proteomic studies of the atherosclerotic plaque were carried out in the past (de la Cuesta et al., 2013; Hao et al., 2014), but the proteomics of the vascular injury still remains not fully understood. The plasticity of VSMC in modulating their phenotype and their subsequent proliferation and migration have been implicated in atheroma or intimal hyperplasia after vascular injury (Boccardi et al., 2007). Boccardi et al identified 105 proteins that were down - and 154 that were up-regulated in activated-proliferating VSMC compared to the quiescent one. They also documented a decreased phosphorylation level shortly right after stimulation with a quick recovery and showed the implication of chaperones, redox-related enzymes and cytoskeleton components such as α_1-actin in the alteration process (Boccardi et al., 2007). Kang et al identified 27 proteins which play a role in VSMC phenotype modulation, with oxidized LDL receptor-1 (OLR1) playing a dual role in VSMC hyperplasia by directly mediating monocyte adhesion and by assisting the PDGF-induced proliferation/migration (Kang et al., 2015). Survivin is another identified protein that plays a key role in vascular remodeling. It regulates the proliferation and

apoptosis of VSMC via the PDGF pathway and was found to be upregulated seven days after injury (Wang et al., 2005). Its inhibition after injury resulted in a suppression of neointima formation by 63 % (Blanc-Brude et al., 2002).

Our group performed a deep proteomics analysis after wire-induced vascular injury of femoral arteries and discovered significant differences in expressed proteins between injured and non-injured femoral arteries (4,836 vs. 3,349) at different time-points by using single run high-resolution MS, where more than a half of them were either up- or downregulated at day three after injury (Wierer et al., 2021). Using Gene Ontology (GO) enrichment analyses, it was shown that the upregulated proteins were implicated in different pathways, including those related to cell adhesion, cell activation, immune response, ECM, migration and proliferation, with the last three showing the most prominent proteomic changes. Among others, different migration factors (e.g. Ptprc, Myo1g, Itga11, Itga2b) and surface markers (e.g. Cd34, Cd44, Cd47) were found to alter their expression in response to injury. In particular, low abundant migration factors such as Itga11, Elane and the transient receptor potential channel 6 (Trpc6) ion channel were found to be expressed only after injury (Wierer et al., 2021). TRPC6 was previously associated as the calcium channel mediating the increased cytosolic free Ca^{2+} ion concentration required for migration in breast cancer cell lines (Jardin et al., 2018), leukocyte transendothelial migration (Weber et al., 2015) and for chemotaxis of murine neutrophils (Lindemann et al., 2013).

1.2.2 TRPC6

TRPC6 is part of the transient receptor potential (TRP) channels, which were first described in *Drosophilia melanogaster*. The form “transient receptor potential” derives from the observation of the photoreceptors carrying TRP gene mutations which exhibited a transient voltage response to continuous light (Montell et al., 1985). Mammalian TRP channels are ubiquitously expressed in diverse tissues and different cell types and their family consists of six main subfamilies based upon their amino acid sequence homology: the TRPC (canonical), TRPV (vanilloid), TRPM (melastatin), TRPP (polycystin), TRPML (mucolipin) and the TRPA (ankyrin) groups (Nilius et al., 2007).

The TRPC subfamily, which are termed ‘canonical’ because they are most closely related to *Drosophilia* TRP, consists of seven different members, i.e. TRPC1-7. Each

TRP channel subunit has six transmembrane spanning domains (S1–S6), with a reentering loop between the fifth and the sixth transmembrane domain lining the pore (**Figure 2**). Both Carboxy- and Amino-termini are located intracellularly. They form homo- or heterotetramer functional complexes with the other members of the TRPC subfamily (Clapham et al., 2001; Hofmann et al., 2017). TRPC6 has four ankyrin repeats (Ank) near the Aminoterminus, followed by a terminal coiled-coin (cc) domain (**Figure 2**). On the other side, distal to the transmembrane fragments is located the TRP domain, which is followed by a calmodulin and inositol triphosphate (IP3) receptor-binding region (CIRB region). A cc domain and the Carboxyterminus follows (Dryer & Reiser, 2010).

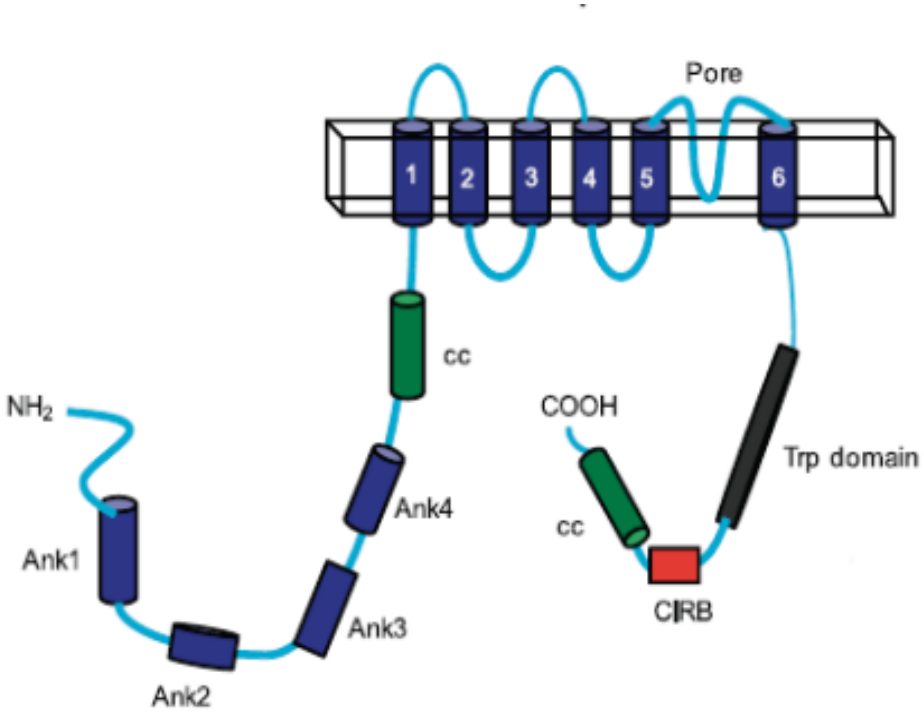

Figure 2: TRP channel structure. For details please see text NH2, Aminoterminus; Ank, Ankyrin repeats; cc, coiled coin domain, COOH, Carboxyterminus; CIRB, calmodulin and inositol triphosphate (IP3) receptor-binding region, Adapted by permission from The American Physiological Society: Figure 1 from Renal Physiology 2010, 299(4):F689-F701 (Dryer & Reiser, 2010) copyright © 2010

TRPC6 is a non-selective calcium permeable channel, shows a tightly receptor operated behavior and has a similar structure to other TRP channels (Dietrich & Gudermann, 2007). It was shown that TRPC6 has a six-time higher permeability for Ca^{2+} over Na^{+} (Dietrich et al., 2003; Hofmann et al., 1999).

Ca^{2+} acts as a second-messenger in many physiological events and Ca^{2+} signals are generated through various mechanisms. These include plasma membrane voltage-operated Ca^{2+} entry, Ca^{2+} liberation from intracellular stores and store-operated Ca^{2+} entry following intracellular stores depletion [for an overview see (Berridge, 2012; Clapham, 1995; House et al., 2008)]. The focus of this work will be calcium influx following phospholipase C (PLC) activation, often described as receptor-operated Ca^{2+} currents (ROC).

Elevation of the cytosolic Ca^{2+} concentration is seen as a growth stimulus for SMC and associated with their increased proliferation and migration (Berridge, 1995). Ligands such as hormones, neurotransmitters and growth factors can raise the intracellular Ca^{2+} concentration by binding to a specific receptor (G-coupled- or tyrosine kinase receptor) at the cell membrane, which leads to activation of one of the various isoforms of PLC (**Figure 3)** (House et al., 2008; Mori et al., 2015).

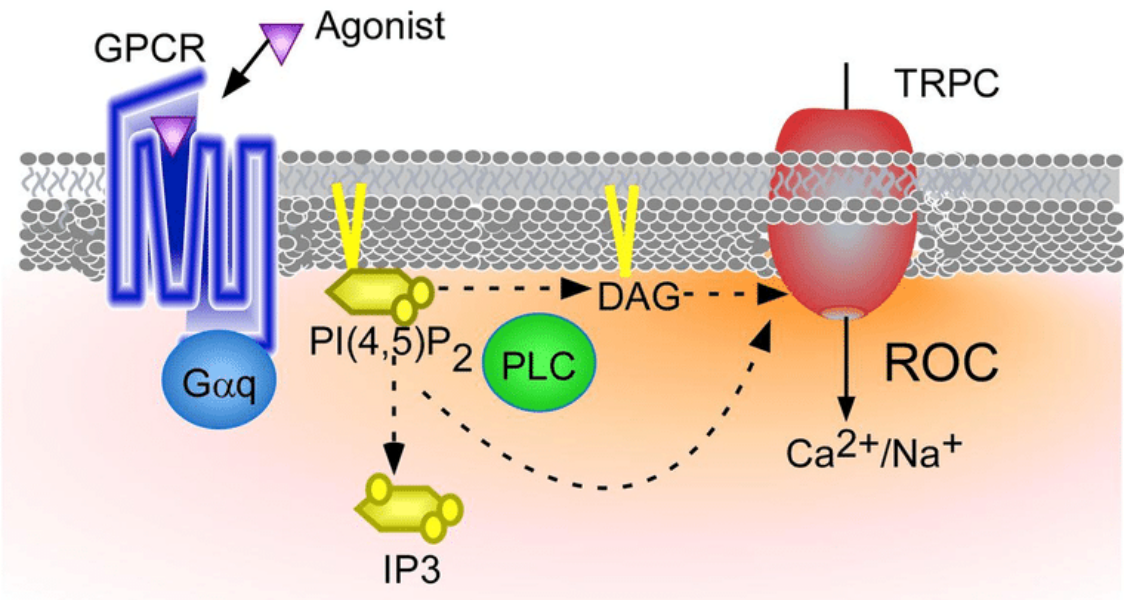

Figure 3: TRPC as receptor operated calcium current (ROC): Activation of PLC following the binding of an agonist to GPCR leads to the generation of IP3 and DAG by cleaving the membrane-bounded PI(4,5)P2. Calcium influx is triggered into the cytoplasm by activation of TRPC channel by DAG and by binding of IP3 to the IP3 receptor on the endoplasmatic reticulum (ER) membrane. GPCR, G-protein coupled receptor; $PI(4,5)P_2$, phosphatidylinositol-4,5-bisphosphate; DAG, diacylglycerol; IP3, inositol-1,4,5-trisphosphate; PLC, phospholipase C; TRPC, transient receptor potential canonical channel. Reproduced by permission from Mori et al., 2015: Figure 1 from Front. Pharmacol. 2015, 6:22 (Mori, Itsuki, Hase, Sawamura, Kurokawa, Mori and Inoue, 2015) copyright © 2015

PLC has a particularly affinity for inositol lipids of the cell membrane and is responsible for cleaving phosphatidylinositol-4,5-bisphosphate ($PI(4,5)P_2$) into the membrane-bound diacylglycerol (DAG) and soluble inositol-1,4,5-trisphosphate (IP_3) (**Figure 3**). DAG activates the TRPC6 ion channel, which triggers calcium influx into the cell cytoplasm (Hofmann et al., 1999). TRPC channel activity can also be modulated by binding of IP_3 to its IP_3 receptor, which causes a liberation of Ca^{2+} from intracellular stores (Clapham et al., 2001). TRPC subfamily is divided in two main groups based on structural and functional similarities: a) TRPC1/4/5, which are not sensitive to DAG and b) TRPC3/6/7, which are activated by DAG (Xie et al., 2012).

The exact physiological role of TRPC6 is still unknown. A biological relevance of TRPC6 has been shown in the brain where TRPC6 is believed to promote hippocampal neuron dendritic growth (Tai et al., 2008), while inhibition of its degradation suppressed ischemic brains damage in rats (Du et al., 2010). In the kidney, TRPC6 was shown to be associated with the development of focal segmental sclerosis (FSGS) [reviewed in (Dietrich et al., 2010)]. In the vasculature, TRPC6 is one of the most commonly expressed TRP channels (House et al., 2008). In the heart, overexpression of Trpc6 in transgenic mice was found to induce pathologic cardiac hypertrophy in *vivo*, facilitating the transition to cardiomyopathy (Kuwahara et al., 2006). In vein myocytes, TRPC6 suppression was shown to reduce the store depletion-independent CA^{2+} influx through the α_1-adrenoreceptor-activated nonselective cation channels (α_1-AR-NSCC) (Inoue et al., 2001). In addition, TRPC6 was shown to be a molecular correlate of vasopressin induced Ca^{2+} entry in VSMC (Jung et al., 2002). Moreover, its upregulation was linked to enhanced PDGF-induced SMC proliferation (Yu et al., 2003).

1.3 Aim of this study

TRPC6 is a cation channel involved in capacitative and receptor-operated calcium entry in the cell. Using deep proteomic profiling of injured murine femoral arteries, our research group identified Trpc6 to be upregulated in the early phase after vascular injury, i.e. Trpc6 was transiently upregulated. This study aimed to answer the following questions:

1. What is the consequence of activating or blocking TRPC6 in VSMC regarding proliferation/migration?
2. Does Trpc6 deficiency lead to reduced neointima formation *in vivo*?
3. Does genetically altered *TRPC6* expression influence the risk of restenosis after coronary stenting?

2 Material

2.1 Chemicals

Table 1 List of chemicals used

Chemical	Catalogue#	Manufacturer	Headquarters
1-Oleoyl-2-acetyl-sn-glycerol (OAG)	O6754	Sigma Aldrich	St. Louis, USA
10X RIPA	9806S	New England Biolabs	Ipswhich, USA
10X TRIS/glycine/SDS	161-0772	Bio-Rad	Hercules, CA, USA
2-propanol ROTIPURAN® ≥ 99.8 %	6752	Carl Roth	Karlsruhe, Germany
4X laemmli	1610747	Bio-Rad	Hercules, CA, USA
β-mercaptoethanol	M3148	Sigma Aldrich	St. Louis, USA
dimethyl sulfoxide (DMSO)	A3672	AppliChem	Darmstadt, Germany
EMPURA® ethanol absolute	1070172511	Merck Millipore	Bellerica, USA

Chemical	Catalogue#	Manufacturer	Headquarters
Eosin Y solution 0.5 % in water	X883.2	Carl Roth	Karlsruhe, Germany
Ethanol denatured ≥ 96 %	T171	Carl Roth	Karlsruhe, Germany
formaldehyde solution 4 % for Histology	A3697	AppliChem	Darmstadt, Germany
Gelatin-Based Coating Solution- ready to use	PB-6950	PELOBiothec, GmbH	Planegg, Germany
Gibco™ PBS (10X), pH 7.4	70011044	Thermo Fisher Scientific	Waltham, USA
Gibco™ trypan blue solution, 0.4 %	15250061	Thermo Fisher Scientific	Waltham, USA
Glycine PUFFERAN® ≥ 99 %	3908	Carl Roth	Karlsruhe, Germany
Hemalum solution acid acc. to Mayer	T865.3	Carl Roth	Karlsruhe, Germany
HEPES buffered saline solution	C-40020	PromoCell	Heidelberg, Germany
Hydrochloric acid (HCl), 6 mol/l - 6 N	281	Carl Roth	Karlsruhe, Germany
Methanol (MeOH)	131091	AppliChem	Darmstadt, Germany

Chemical	Catalogue#	Manufacturer	Headquarters
Nonfat dry milk powder BioChemica	A0830	AppliChem	Darmstadt, Germany
Penicillin-streptomycin 10,000 units penicillin/ml, 10 mg streptomycin/ml)	P4333	Sigma Aldrich	St. Louis, USA
Pertex® Mounting medium	41-4011-00	Medite GmbH	Burgdorf, Germany
SAR7334 5 mg	5831	Tocris Bioscience	Bristol, UK
SmBM™ Smooth Muscle Cell Basal medium	CC-3181	Lonza	Basel, Switzerland
SmGM™- 2 Smooth Muscle medium-2 SingleQuots Kit	CC-4149	Lonza	Basel, Switzerland
smooth muscle cell growth medium 2	C-22062	PromoCell	Heidelberg, Germany
smooth muscle cell growth medium 2 Supplement mix	C-39267	PromoCell	Heidelberg, Germany
TRIS PUFFERAN® ≥ 99.9 %	4855	Carl Roth	Karlsruhe, Germany

Chemical	Catalogue#	Manufacturer	Headquarters
Trypsin-EDTA (0.04 %/0.03 %)	C-4120	PromoCell	Heidelberg, Germany
Trypsin neutralising solution (0.05 % trypsin inhibitor in 0.1 % BSA)	C-41120	PromoCell	Heidelberg, Germany
Tween® 20 *BioChemica*	A1389	AppliChem	Darmstadt, Germany
Xylene (isomers), 2.5 l, glass	9713.3	Carl Roth	Karlsruhe, Germany

2.2 Buffers, media and solutions

Standard buffers and solutions

1X phosphate buffered saline (PBS)

Final concentration of 1 mM KH_2PO4, 0.16 M NaCl, 2.97 mM Na_2HPO_4-7H2O, pH 7.4 at room temperature

100 ml 10X Gibco™ PBS (Thermo Fisher Scientific)

ad 1000 ml Millipore® water

stored at room temperature

Buffers and solutions for histology

0.1 % HCL-Solution

15 ml HCL (2 mol)

ad 1000 ml Millipore® water

stored at room temperature

70 % v/v ethanol

350 ml EMPURA® ethanol absolute (Merck Millipore)

ad 500 ml Millipore® water

stored at room temperature

Solution and media for the cultivation of cells

VSMC medium (Promocell)

500 ml smooth muscle cell growth medium 2 (PromoCell)

25 ml smooth muscle cell growth medium 2 SupplementMix (PromoCell)

5 ml penicillin-streptomycin (Sigma-Aldrich)

stored at 4 °C

10 % DMSO (AppliChem) was added to the cell line media to freeze cells

Solution and buffers for Western blot

1X radioimmunoprecipitation assay (RIPA) buffer

10 ml 10X RIPA (New England Biolabs)

ad 100 ml Millipore® water

stored at - 20 °C

4X laemmli buffer

with a final concentration of 355 mM β-mercaptoethanol

100 µl β-mercaptoethanol (Sigma-Aldrich)

900 µl 4X laemmli (Bio-Rad)

stored at - 20 °C

1X running buffer

100 ml 10X 10X Tri/Glycine/SDS (Bio-Rad)

2 ml Tween® 20 (AppliChem)

ad 1000 ml Millipore® Water

stored at room temperature

1X transfer buffer

3.03 g TRIS PUFFERAN® (Carl Roth)

14.4 g glycine PUFFERAN® (Carl Roth)

0.2 l methanol (AppliChem)

ad 1,000 ml Millipore® water

stored at room temperature

1X PBS-T

Final concentration of 1 mM KH_2PO_4, 0.16 M NaCl, 2.97 mM Na_2HPO_4-7H2O, 0.2 % v/v Tween® 20, pH 7.4 at room temperature

100 ml 10X Gibco™ PBS (Thermo Fisher Scientific)

2 ml Tween® 20 (AppliChem)

ad 1,000 ml Millipore® water

stored at room temperature

5 % w/v milk in PBS

5 g nonfat dry milk powder (AppliChem)

ad 100 ml 1X PBS (diluted from 10X Gibco™ PBS in Millipore® water)

stored at 4 °C for up to two days

2.3 Cell lines

VSMC were commercially available and purchased from PromoCell.

Table 2 Commercially available cell line

Cell line	Manufacturer	Headquarters	Order#
human vascular smooth muscle cells	PromoCell	Heidelberg, Germany	C-12533

2.4 Antibodies

2.4.1 Primary antibodies

The primary antibody, the anti-TRPC6 antibody (rabbit AK 861 affinity purified, 1:200) was kindly provided by Professor Veit Flockerzi (University of Saarland).

2.4.2 HRP-conjugated secondary antibodies

Table 3 HRP-conjugated secondary antibodies used

Antibody	Manufacturer	Headquarters	Order#
anti-rabbit IgG, HRP-linked antibody	Cell Signaling Technology	Danvers, MA, USA	7074

2.5 Mice

Eight to 12 weeks old mice from the C57BL/6J strain were obtained from Jackson Laboratories, Bar Habor, ME, USA. They were fed with a standard ssniff® diet and kept in Makrolon® cages type III H.

2.6 Compounds used

Table 4 List of used compounds

Active substance	Concentration	Dosage	Name	Manufacturer	Headquarters
Buprenorphine	0.3 mg/ml	0.05 mg/kg	Temgesic®	RB Pharmaceuticals Limited	Berkshire, UK
Sodium chloride	0.90 %		isotonische Natriumchloridlösung 0.90 %	AlleMan Pharma	Pfullingen, Germany
Pentobarbital sodium	300 mg/ml	600 mg/kg	Release®	WDT	Garbsen, Germany

2.7 Commercially available kits

Table 5 List of commercially available kits

Kit	Manufacturer	Headquarters	Article#
Pierce™ BCA protein assay kit	Thermo Fisher Scientific	Waltham, USA	23225
Pierce™ ECL Western blotting substrate	Thermo Fisher Scientific	Waltham, USA	32106
Cell Proliferation Elisa BrdU (colorometric)	Roche, Applied Science	Penzberg, Germany	11647229001

2.8 Devices and utensils

Table 6 List of used devices and utensils

Manufacturer's type designation	Device	Manufacturer	Headquarters
AP 280-2 Paraffin Wax Cool/Heat PARTS	Tissue embedding center	Microm	Walldorf, Germany
Culture Cylinder (ID 2 mm, Height 5 mm)	Culture cylinder	Bioptechs	Butler, PA, USA
HM 340E Electronic Rotary Microtome	Paraffin Section's cutter	Thermo Fisher Scientific	Waltham, USA
Infinite® M200 Pro	microplate reader	Tecan Group	Männedorf, SUI
ImageQuant™ LAS 4000	biomolecular imager	GE Healthcare Life Sciences	Chicago, IL, USA
Leica DMRB	Fluorescence Microscope	Leica Mikroskopie & Systeme GmbH	Wetzlar, Germany
Milli-Q® Reference	Water purification system	Merck Millipore	Billerica, USA
Mini-PROTEAN® tetra cell	vertical gel electrophoresis	Bio-Rad	Hercules, USA
Mini Trans-Blot® electrophoretic transfer cell	blotting module	Bio-Rad	Hercules, USA

Manufacturer's type designation	Device	Manufacturer	Headquarters
PowerPac™ Basic Power Supply	power supply	Bio-Rad	Hercules, USA
Stemi 200C	Stereo Microscope	Zeiss	Oberkochen, Germany
Stretching Table OTS 40	Tissue samples dryer and stretcher	Medite GmbH	Burgdorf, Germany
STP 120 Spin Tissue Processor	tissue processor	Microm	Walldorf, Germany
Tissue cool plate, COP 30	cooling plate	Medite GmbH	Burgdorf, Germany
Tissue Floatation Bath TFB 45	tissue water bath	Medite GmbH	Burgdorf, Germany
Wheaton™ Micro Tissue Grinder With Cap, PTFE Pestle and Cap Liner	tissue grinder	Thermo Fisher Scientific	Waltham, USA
Zeiss Axiovert 100	Phase Contrast Microscope	Zeiss	Oberkochen, Germany
Zeiss Axiocam HRc	Microscope camera	Zeiss	Oberkochen, Germany

2.9 Software

Table 7 List of software used

Software	Application	Manufacturer	Headquarters
GraphPad Prism® software version 8.0.1 for Mac OS X	Statistical analyses	GraphPad Software	La Jolla, Ca, USA
iControl v1.10	Proliferation Assay	Tecan Group	Männedorf, SUI
ImageJ 1.47v	Scratch Assay Morphometric analyses	National Institute of Health	Bethesda, USA
ImageQuant™ LAS 4000 v1.2	Western Blot	GE Healthcare Life Sciences	Chicago, USA
ImageQuant™ TL 1D v8.1	Western Blot	GE Healthcare Life Sciences	Chicago, USA
Magellan™ data analysis software v7.2	BCA measurement	Tecan Group	Männedorf, SUI
Zen lite 2012	Cell culture	Zeiss	Oberkochen, Germany

3 Methods

3.1 Animal experiments

In this study, we used the mouse for studying neointima formation. All performed animal experiments were done by registered veterinarians, in line with the approved protocols of the international guidelines and under the permission of the government of Upper Bavaria (55.2-1-54-2532-17-14). For the experiments, mice of the C57BL/6J strain were used. Trpc6-deficient mice ($Trpc6^{-/-}$) were generated as previously described (Dietrich et al., 2005). As control animals served mice from the same colony, which originated from the breeding of the heterozygous Trpc6-Knockout-mice. They are referred to as wild type (wt) in the following text.

To study neointima formation, we performed a wire-induced femoral artery injury in eight to 12 weeks old mice as described by Sata et al (Sata et al., 2000) and studied neointima formation after 28 days. A dissection microscope (Stemi200C, Zeiss, Germany) was used for performing surgery. After reaching the stage of surgical anesthesia, a skin incision was made. The left femoral artery was bluntly dissected and separated from the femoral nerve. Both the femoral vein and the femoral artery were looped distally and proximally with a 7/0 polypropylene suture, which served as a tourniquet for vascular controlling. The deep femoral artery branch of the femoral artery served as transverse arteriotomy wire entrance, which runs between the pectineus and the adductor longus muscle. The branch was distally ligated and after stopping the blood flow, a 0.38 mm (No. C-SF-15-15, COOK, Bloomington, IN) wire was inserted into the femoral artery and advanced toward the iliac artery. The wire was placed for one minute (min) in the vessel to denude and dilate the artery. After injury, the wire was removed and the blood flow restored. Postoperative pain control was achieved by subcutaneous injection of Buprenorphine (0.05 mg/kg of body weight) (RB Pharmaceuticals Limited, Berkshire, UK) every eight hours in a period of 72 hours.

Mice were sacrificed after three, seven, 14, 28 days by intraperitoneal injection of pentobarbital (600 mg/kg) (WDT, Garbsen). In order to get rid of the blood from the femoral arteries, 20 ml of 0.9 % NaCl solution was administered via the left ventricle followed by the perfusion fixation of 4 % paraformaldehyde in Phosphate-buffered saline (PBS) over the descending aorta. Both femoral arteries (injured and non-injured) were

cut out and snap-frozen stored in liquid nitrogen at – 80 °C until fixation with 4 % paraformaldehyde for histological analysis took place.

3.2 Immunoblotting

Western Blot is an analytical technique in molecular biology, which produces semi-quantitative and qualitative data regarding a protein of interest. In this study, it was used to validate TRPC6 protein expression in non-injured and injured (three, seven or 14 days) femoral arteries of C57BL/6J mice, shown in the LC-MS/MS analyses.

3.2.1 Protein isolation from femoral arteries

To isolate the protein from the snap-frozen femoral arteries, the tissue was first grinded manually using a Homogenizer (Thermo Fisher Scientific, Waltham, USA). Protein isolation was done on ice. Cell lysis was performed by adding 1X 40 µl radioimmunoprecipitation (RIPA) buffer (New England Biolabs, Ipswhich, USA). To break all cell clusters, sonication was done three times for 30 sec until the lysate became clear. During sonication, the samples were kept on ice. After centrifugation for 10 min at 4 °C and 6,000 rpm, the pellet containing the cellular debris was discarded and supernatants were stored at - 80 °C for further experimentation.

3.2.2 Protein quantification

Protein concentration was measured using the Pierce™ BCA protein assay kit (Thermo Fisher Scientific). The principle of this method is that proteins can reduce Cu^{2+} to Cu^{+} in an alkaline solution (also known as the biuret reaction). The amount of reduction is proportional with the amount of the protein present. Bicinchoninic acid (BCA) binds Cu^{+} and forms a purple-blue complex in alkaline environments. The BCA assay was performed at 37 °C in a 96-well microplate and measurements were done at 562 nm using the Infinite® M200 PRO microplate reader (Tecan Group).

3.2.3 Western Blots

Immunoblotting, also known as Western blotting, is a commonly used method to detect specific proteins by using the specificity of an antibody-antigen interaction (Mahmood & Yang, 2012). In brief, proteins are separated according to their size using sodium dodecyl sulfate polyacrylamide gel electrophoresis (SDS-PAGE). They are then transferred to a nitrocellulose membrane (Merck Millipore, Billerica, USA) and subsequently detected using specific antibodies on the surface of the membrane.

Sample preparation: Cell lysates were mixed with RIPA and 12.5 µl 4x Lammli-buffer (Sigma-Aldrich, St. Louis, MO, USA), which contains sodium dodecyl sulfate (SDS) and β-mercaptoethanol (BME), in a sterile 1.5-ml tube to a maximum volume of 50 µl. To denaturate proteins and to allow binding of SDS, the samples were boiled for five min at 95 °C using a Thermocycler (Thermo Fisher Scientific, Waltham, USA).

Protein separation by SDS-PAGE: 10 µg of each sample was first loaded into the wells of the SDS-PAGE gel using Mini-PROTEAN Tetra Cell electrophoresis system (Bio-Rad Laboratories, Hercules, CA, USA). A 4 - 20 % gradient gel was used for the protein separation. Gel was run for five min at 50 V. Afterwards the voltage was increased to 150 V and the run was finished in about 1 hour.

Membrane transfer (Wet Transfer): Transfer was done using a western blotting transfer system (Trans-Blot® Turbo, Bio-Rad Laboratories, Hercules, CA, USA) according to the manufacturer's instructions to a nitrocellulose membrane at 100 V for 1.5 hours.

Immunoblotting: In order to prevent nonspecific binding of the antibodies to the membrane, samples were blocked with 5 % low-fat milk for one hour. The membrane was then washed three times with PBS-T 20 % and incubated at 4 °C overnight with the primary anti-Trpc6 antibody (rabbit AK 861 affinity purified, 1:200, kindly provided by Professor Veit Flockerzi, University of Saarland).

Detection: Before application of the anti-rabbit IgG-HRP linked secondary antibody (Cell Signaling Technology, Danvers, MA, USA, 7074S, 1:100,000), the membrane was washed with PBS-T three times for five min each. One hour after adding the secondary antibody at room temperature, the membrane was rinsed three times for 10 min with PBS-T and subsequently incubated in a chemiluminescence substrate

(Thermo Fisher Scientific Super Signal West Dura Extended Duration Substrate; Life Technologies, Carlsbad, CA, USA).

Image and analysis: Chemiluminescence was detected with an ImageQuant LAS 4000 (GE Healthcare Life Sciences, Pittsburgh, PA, USA) imager. Analysis was done using ImageQuant TL 1D v8.1 (GE Healthcare Life Sciences, Pittsburgh, PA, USA). In order to compare our target protein expression levels between several different samples, signal intensities were normalized to signal intensities for Glyceraldehyde 3-phosphate dehydrogenase (GAPDH) in the according samples. This was done by dividing the band volume of the target protein by the band volume of the control GAPDH.

3.3 Cell culture

All solutions (Medium, PBS, HEPES, trypsin-EDTA) were pre-warmed to 37 °C before usage by using a water bath. Experiments were performed under a horizontal laminar flow cabinet.

Cell culture flasks and well plates coating: Cell culture dishes were coated with gelatin solution (Pelobiotech GmbH, Planegg, Germany) and left at room temperature for 30 min. Coating was done by using five ml of gelatin for a T175 cell culture flasks and 500 µl per well for a 24 well plate. Before seeding, the gelatin solution was aspirated.

Defrosting of frozen cells: T175 cell culture flasks were first labeled with cell line name, passage number and date of defrosting. A frozen vial of VSMC was collected from the liquid nitrogen storage and transferred to the laboratory on an ice box to a 37 °C pre-warmed water bath, where the cells were kept for one to two minutes to allow them to thaw out. Once thawed, the whole content of the vial was pipetted into a 15-ml sterile tube and five ml of pre-warmed medium was added slowly. Subsequently, the cell suspension was transferred to a flask and 10 more ml of pre-warmed media was added to achieve the cell seeding density. After that, cells were incubated at 37 °C in a 5 % CO2 humidified incubator. Medium was first changed after 24 hours to remove the cryoprotectant DMSO and then refreshed every two to three days.

Subculturing cells: Subculturing was performed once the cells had reached 70 - 80 % confluency. Spent medium was removed and the cells were washed with HEPES

(Promocell). 0.04 % Trypsin-EDTA (Promocell) was used for the trypsinization and the flask was returned to the incubator and left there for three to four min. Immediately after the incubation period at 37 °C, cells were examined under the microscope. Once detached, trypsin neutralizing solution (Promocell) was added in a ratio of 1:2 to inactivate the trypsin. Shortly after, the cell suspension was transferred to a 50-ml sterile tube and centrifuged at 1000 x g for two min. After the removal of the supernatant, cells were resuspended in fresh pre-warmed culture media and then counted and transferred either to new labelled flasks or to multiwell plates (see Table 8 for the cell number seeded).

Table 8 Cell number seeded

Cell type	24 well plates (500 µL)	96 well plates (100 µL)
VSMC	100,000/well	10,000/well

Cell Quantification: Cells were brought into suspension as previously described. 10 µl of the cell suspension was removed and the equal volume of 0.4 % Gibco™ trypan blue solution (Thermo Fisher Scientific) was added and then mixed by gentle pipetting. After cleaning the Neubauer hemocytometer, the coverslip was moistened with exhaled breath and slid back and forward over the chamber under little pressure until it got stuck. Both sides of the chamber were then filled with cell suspension and viewed under one phase microscope using 10x magnification. Viable cells were counted and their concentration was calculated.

Cryopreservation of cells: Cells were trypsinized and counted as described. They were then centrifuged at 1000 x g for three min and resuspended at a concentration of 0.5 - 1 x 10^6 cells/ml in freeze medium. One ml of cell suspension was pipetted into cryoprotective ampoules and kept for 24 hours in a with isopropanol (100 % v/v) filled box before placing them for long-term storage in liquid nitrogen.

3.4 VSMC migration assays

To measure the migration of VSMC in vitro, we performed two different migration assays, i.e., scratch wound healing assay and migration radius assay.

3.4.1 Scratch wound healing assay

For the scratch wound assay, cells were seeded in 24 well plates at a density of 100,000 cells per well. After 24 hours of growth, when they reached a confluency of 70 – 80 % as a monolayer, a 200 µl pipette tip was used to make a vertical wound down through the cell monolayer, with the tip's long axis being perpendicular to the bottom of the well during the scratch. The media and cell debris were carefully aspirated and the cells gently washed twice with PBS. The wells were then replenished with fresh growth medium supplemented with 1-Oleoyl-2-acetyl-sn-glycerol (OAG) (Sigma-Aldrich, St. Louis, MO, USA) at final concentration of 100 µM or SAR7334 (Tocris Bioscience, Bristol, UK) at a final concentration of 100 nM. OAG was activated by sonication before use. As controls, served wells replenished with growth medium and DMSO at a final concentration of 1 %. Cells were then incubated at 37 °C and pictures were acquired directly after the scratch (t0), after six hours (t1), eight hours (t2) and 12 hours (t3) using a phase-contrast microscope with a camera (Zeiss Axiovert 100 and Zeiss Axiocam HRc, Zeiss, Oberkochen, Germany). Zen lite 2012 Software (Zeiss, Oberkochen, Germany) was used to save the pictures. Wound area was quantitatively evaluated by using the ImageJ version 1.47v software and the wound reclosure was measured as Δt0-t1-3, depicted as 10^3 pixels and the mean value was calculated. Measurements were performed in triplicates and at least five from each other independently experiments were done.

3.4.2 Migration radius assay

For the migration radius assay, we used culture cylinders (Bioptechs, Butler, PA, USA) with a total and inner diameter respectively of four and two mm, which were placed in the middle of the well of 24 well plates. The culture cylinders were first coated for 30 min at room temperature with gelatin solution (Pelobiotech GmbH, Planegg,

Germany), which was aspirated before cell seeding. Cells were seeded around the cylinders at a density of 100,000 cells per well. The inner area of the cylinders was filled up with 20 µL of SAR7334 with a final concentration of 100 nM in gelatin. As controls served the equal volume of DMSO with a final concentration of 1 %. The cells were then incubated for 24 hours at 37 °C in a 5 % CO2 humidified incubator. After that, the cylinders were removed and pictures were immediately taken (t0). The cells were incubated at the same conditions for another 24 hours and pictures were again acquired (t1: 48 hours after seeding). The acquisition of the pictures was done using a phase-contrast microscope with a camera (Zeiss Axiovert 100 and Zeiss Axiocam HRc, Zeiss, Oberkochen, Germany). The wound reclosure was measured as Δt0-t1 (48 hours), depicted as 10^3 pixels and the mean value was calculated. Measurements were performed in duplicates and at least five from each other independent experiments were done.

3.5 VSMC proliferation assays

Cell Proliferation ELISA, BrdU (colorimetric) from (Roche, Applied Science, Penzberg, Germany) was used for the quantification of cell proliferation based on the measurement of the pyrimidine analogue BrdU incorporation instead of thymidine during DNA synthesis. It was performed according to the manufacturer's instructions. Cells were seeded in 96 well plates at a density of 10,000 cells per well in 100 µl starving medium (i.e. without growth factors and FBS) and incubated at 37 °C for 24 hours. After that, starving medium was aspirated and the wells were replenished with growth medium which was either supplemented with OAG (Sigma-Aldrich, St. Louis, MO, USA) at a final concentration of 100 µM or SAR7334 (Tocris Bioscience, Bristol, UK) at a final concentration of 100 nM. Growth medium supplemented with DMSO at a final concentration of 1 % served as vehicle. The cells were incubated at 37 °C for another 24 hours, before 10 µl/well of BrdU labeling solution was added. After the addition of BrdU, cells were reincubated for additional 24 hours at 37 °C. Using the iControl v1.10 software, the absorbance was measured at 370 nm with a reference wavelength of 492 nm in the Infinite® M200 PRO microplate reader (both Tecan Group, Männedorf, Switzerland). Measurements of each sample and control were performed in triplicates and at least five independent experiments were done. A blank control, which provided information about the unspecific binding of BrdU and anti-BrdU to the multiwell plate, was performed at each experiment.

3.6 Histological analysis

Following dissection of the femoral arteries, the tissue samples were fixed. Fixation helps to maintain the cell and tissue morphology and prevent the autolysis and necrosis of the excised tissues. It was achieved by immersion overnight in 4 % Formaldehyde (Applichem GmbH, Darmstadt, Germany). Dehydration and Paraffinization were carried out automatically using a Spin Tissue Processor (STP-120, Microm, Walldorf). The tissue samples were then embedded in paraffin wax using a Tissue embedding center (AP 280-2, Microm, Walldorf, Germany) and cooled on a cooling plate (Tissue Cool Plate COP20, Medite GmbH, Burgdorf, Germany).

3.6.1 Sectioning

Starting from the distal ligation of the femoral artery, which served as a topographic marker, serial cross-sections of two µm were done using a microtome (HM 340E, Thermo Fisher Scientific, Waltham, MA, USA). The sections were then mounted on microscopy slides (two sections in each slide) and left overnight for drying.

3.6.2 Staining

H&E staining is the most commonly used staining technique in histopathology. As its name suggests, H&E stain makes use of a combination of two dyes, namely hematoxylin and eosin. Hematoxylin has a deep blue-purple color and stains the nuclei dark blue to black, while eosin, which has a pink color, stains the cytoplasm and the ECM red. 10 to 15 sections per femoral artery at 25 µm intervals were stained with HE and embedded in xylene-based mounting medium (Pertex® Mounting medium, Medite GmbH, Burgdorf, Germany). Before starting with the staining procedure, the tissue samples were first deparaffinized and then rehydrated by immersing the slides through the following wells:

a. Xylene: two washes one min each
b. 100 % Ethanol: two washes one min each

c. 96 % Ethanol: one wash for one min
d. 70 % Ethanol: one wash for one min
e. Distilled water: one wash for two min

The H&E-staining was performed according to the following protocol:

1.	Staining with Mayer's Hemalum	three min
2.	Rinse in 0.1 % HCL-Solution	two sec
3.	Differentiate with running tap water	five min
4.	Stain with Eosin-Y-Solution 0.5 %	three min
5.	Rinse in tap water	30 sec
6.	Dehydrate, clear and mount	

The microscopy slides were dehydrated in ascending graded alcohol (Distilled water, 1x Ethanol 70 %, 1x Ethanol 96 %, 2x Ethanol 100 %, 2x Xylene), before mounting them with xylene-based mounting medium.

3.6.3 Microscopy

For the quantification of neointima formation, histological sections of femoral arteries were sectioned and stained as previously described. The images were then blind digitalized at 10x magnification using the Leica-Microscope with a camera (Leica DMRB and Leica DFC450C, Leica Camera AG, Wetzlar, Germany).

3.6.4 Quantification of neointima formation

Digitalized images of stained tissue sections were morphometrically analyzed using image analysis software Image J 1.47v (Schneider et al., 2012). We first measured the areas of the lumen, IEL and EEL. After the calculation of the medial and intimal areas, the neointima/media ratio was estimated.

3.7 Binary restenosis analysis

The analyses of the available data of previous GWAS (Zeng et al., 2019, Nelson et al., 2017) were used for the correlation of rs2513192 genotype with the risk of developing binary restenosis. Our study comprised 4,247 individuals and 6,028 lesions, that were associated with rs2513192 genotype expression. We defined restenosis as the narrowing of the coronary lumen with a cut off value of 50 %. In a sixth month scheduled follow-up angiography, we obtained information about binary restenosis in 3,068 (72.2 %) individuals and 4,279 (71 %) lesions. A patient with a multivessel intervention was analyzed as a restenosis patient by having one or more lesions affected by restenosis at the angiographic follow-up, which was performed approximately six months after the intervention. Patients characteristics and time to angiographic follow-up are illustrated in Table 9. We used a logistic regression model with computation of odds ratio (OR) and 95 % confidence interval (CI) to evaluate if the rs2513192 genotype is linked with the binary restenosis. We included all the variables listed in Table 9 (gender, age, body mass index, insulin-dependent diabetes mellitus, hypertension, hypercholesterolemia, smoking status, positive family history, clinical presentation with acute coronary syndrome or CAD; previous myocardial infarction, CABG or PCI; number of affected coronary vessels, left ventricular ejection fraction, procedural characteristics such as the affected vessels, complete or incomplete occlusions, restenotic lesion, placed stent type and its generation, lesion length, stenosis before and after PCI, total stent length, nominal balloon diameter as wells as the maximal balloon pressure) into the logistic regression. To build a model that avoids overfitting we considered the selection of covariates in the logistic regression. For this purpose, we used the least absolute shrinkage and selection operator regression method after entering all baseline and procedural characteristics as candidates (R package “glmnet”, version 2.0-13).

3.8 Statistical analysis

The distribution of data was estimated using the Kolmogorov-Smirnov test. The data is presented as mean ± SEM, with the normally distributed data being analyzed by using the Student's unpaired/paired test and the not normally distributed data by using the Mann-Whitney-test. For the analyses of the categorical data the chi-square test was used. Statistical significance was assessed by using the GraphPad Prism software version 8.0.1 for Mac OS X (GraphPad Software, La Jolla, CA, USA), with p-values < 0.05 considered as significant.

4 Results

4.1 Validation of increased Trpc6 expression

To validate the transiently increased expression of Trpc6 after vascular injury of murine femoral arteries compared with sham-treated vessels showed in our LC-MS/MS analysis (Wierer et al., 2021), Western Blots were performed. By using an anti-Trpc6 antibody we were able to measure protein amount of Trpc6. We found that Trpc6 protein levels were significantly higher at day three in injured femoral arteries compared to later timepoints and non-injured arteries (**Figure 4**) confirming the results which were obtained by MS.

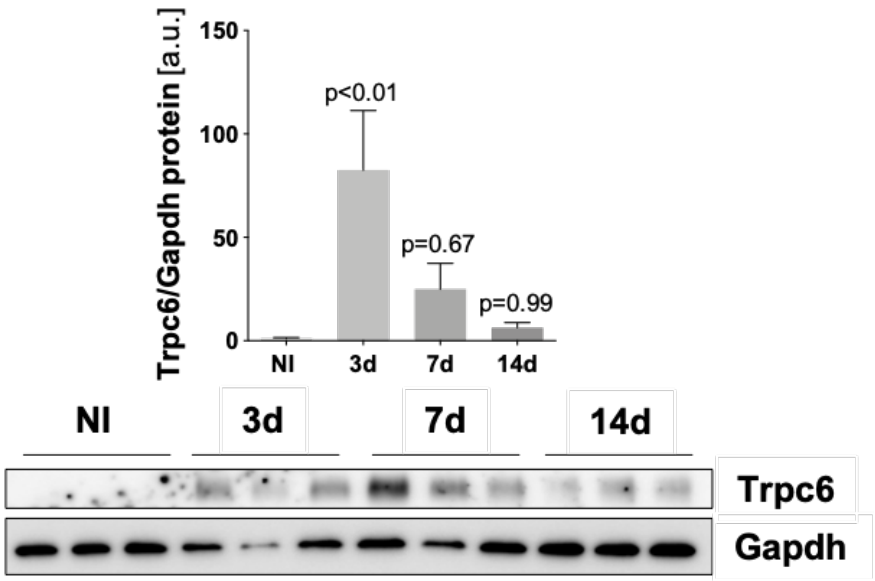

Figure 4: Representative Western Blot showing the expression level of TRPC6 in non-injured femoral arteries (NI) and injured femoral arteries after three (3d), seven (7d) and 14 (14d) days. GAPDH was used as a loading control. Bar graph shows the densitometric analysis in arbitrary units (a.u) of the Western Blot normalized by the housekeeping protein Gapdh. Densitometric values are respresented as mean SEM. Statistical analyses was done with Ordinary one-way ANOVA and Dunnett's multiple comparisons test (3/7/14d vs. NI).

4.2 TRPC6 and VSMC migration

4.2.1 Scratch wound assay

To investigate the role of TRPC6 in VSMC migration *in vitro* we performed scratch wound assays. We first compared cells which were treated with the TRPC6 activator OAG or vehicle and measured wound reclosure after six, eight and 12 hours. We observed enhanced migration of OAG treated VSMC after eight and 12 hours (vehicle 69.05 ± 7.03 vs. OAG 93.09 ± 3.67 [10^3 pixels], p = 0.01 and vehicle 156.93 ± 7.06 vs. OAG 179.14 ± 3.61 [10^3 pixels], p = 0.01, in the given order; **Figure 5A**). Next, we sought to investigate whether TRPC6 inhibition reduces VSMC migration and therefore repeated scratch wound assays in the presence of the TRPC6 inhibitor SAR7334 (Maier et al., 2015). In line with the findings of increased migration after TRPC6 activation, we found that SAR7334 treated VSMC migrated less compared to the vehicle treated VSMC (111.4 ± 15.5 vs. 130.0 ± 10.6 [10^3 pixels], p = 0.04**; Figure 5C**).

4.2.2 Radius migration assay

In addition to the scratch wound assay, we also carried out a radius migration assay to study the local migration of VSMC. For that, with SAR7334 coated dishes were compared with vehicle coated dishes. In line with the scratch wound assay results, we observed a decreased migration of VSMC after coating with SAR7334 after 48 hours (268.2 ± 47.3 vs. 359.2 ± 43.1 [10^3 pixels], p=0.035; **Figure 5D**).

4.3 TRPC6 and VSMC proliferation

We used a colorimetric proliferation ELISA to investigate the effect of inhibiting TRPC6 regarding VSMC proliferation. Using a microplate reader, we measured the wave length absorbance between vehicle and OAG treated cells. We observed an increased proliferation capacity in OAG treated cells in comparison with vehicle (vehicle 0.08 ± 0.03 vs. OAG 0.31 ± 0.07 [absorbance units], p < 0.01; **Figure 5B)**.

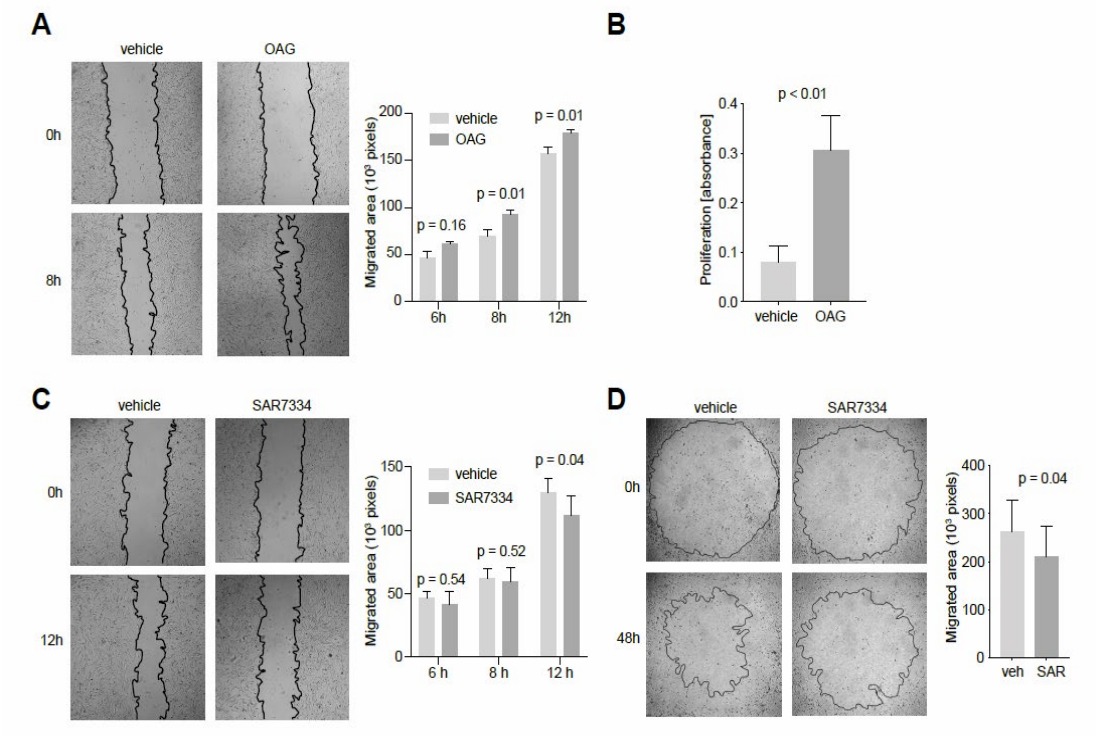

Figure 5: TRPC6 as a novel treatment target in vascular remodeling *A*, Wound scratch assay of human aortic SMC after treatment with 100 µM OAG compared to vehicle and quantification of the reclosure area after six (6h), eight (8h) and 12 (12h) hours (paired t-test) **B**, Measurement of the proliferation capacity of human aortic SMC after treatment with OAG or vehicle by using the cell proliferation Elisa, BrdU (colorimetric) assay (paired t-test) **C**, Wound scratch assay of human aortic SMC after treatment with 100 nM SAR7334 compared to vehicle and the quantification of the reclosure area after six (6h), eight (8h) and 12 (12h) hours (paired t-test) **D,** Radius migration assay of with 100nM SAR7334 coated human aortic SMC compared to vehicle (paired t-test). Data are mean and SEM. At least five independent experiments were done. OAG, 1-oleoyl-2-acetyl-sn-glycerol; h, hours. Reprinted by permission from Oxford University Press: Figure 6 from European Heart Journal 2021. 42(10):1773-1785 (Wierer et al. 2021), copyright © 2021

4.4 Neointima formation in mice lacking Trpc6

To investigate the Trpc6 involvement in the neointima formation *in vivo*, we performed a wire-induced injury of the femoral arteries of Trpc6$^{-/-}$ and wt mice and analyzed the results after 28 days (**Figure 6A).**

In our histological examination, we examined the effect of Trpc6 deficiency by measuring the area of neointima, media and calculating neointima/media ratio after 28 days (**Figure 6B-D**). We observed a reduced neointimal area in Trpc6$^{-/-}$ compared to wt mice (1.90 ± 0.27 vs. 2.82 ± 0.28 [10^4 µm^2], p = 0.03**, Figure 6B**), while the media area

of both genotypes was similar (1.47 ± 0.21 vs. 1.52 ± 0.12 [10^4 µm^2], p = 0.82, **Figure 6C**). In conjunction, we found that the neointima to media ratio was significantly reduced in mice lacking Trpc6 (1.44 ± 0.15 vs. 2.16 ± 0.18, p = 0.01, **Figure 6D**). Our results hence support an implication of Trpc6 in neointima formation in mice.

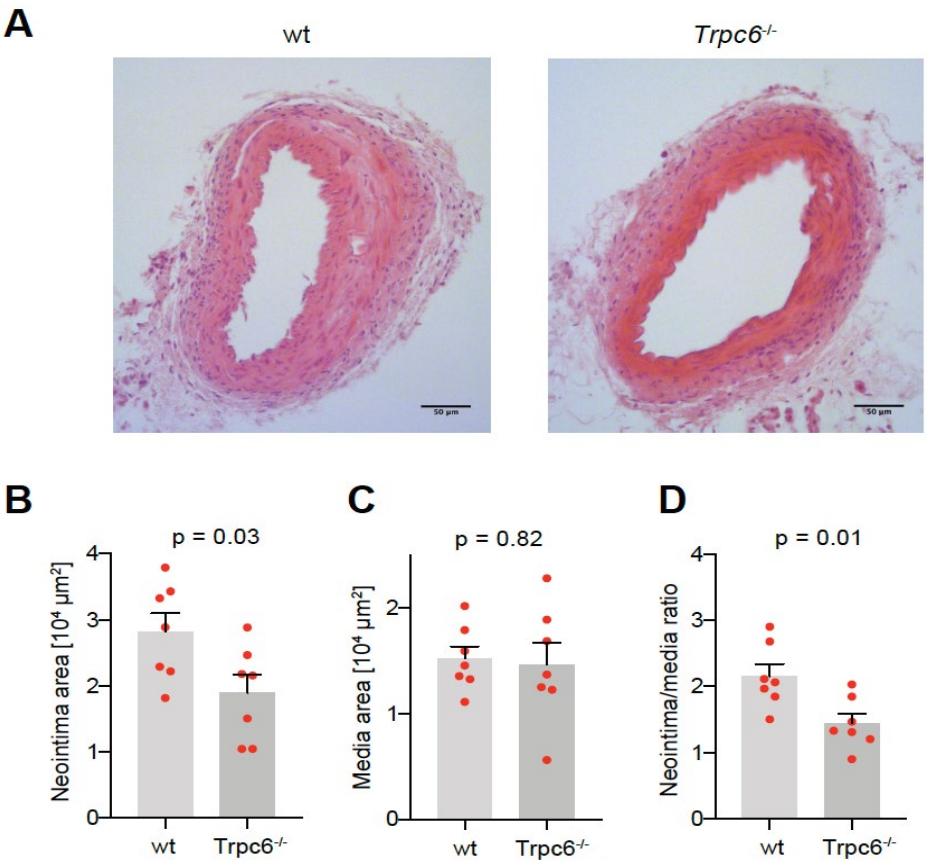

Figure 6: Neointima formation in Trpc6$^{-/-}$ mice. A, H&E staining of femoral arteries 28 days after wire-induced vascular injury in wt and Trpc6$^{-/-}$ mice. **B,** Quantification of the neointima area 28 days after vascular injury in wt and Trpc6$^{-/-}$ mice **C,** Quantification of the media area 28 days after vascular injury in wt and Trpc6$^{-/-}$ mice **D**, Quantification of the neointima/media ratio 28 days after vascular injury in wt and Trpc6$^{-/-}$ mice (unpaired t-test). Data are mean and Standard Error of Mean (SEM). Each symbol represents one mouse. wt, wild type. Reprinted by permission from Oxford University Press: Figure 5 from European Heart Journal 2021. 42(10):1773-1785 (Wierer et al. 2021), copyright © 2021

4.5 *TRPC6* expression and restenosis

We next aimed to investigate if genetically determined *TRPC6* expression influences restenosis following coronary stenting. By querying the GTEX dataset (Consortium, 2013), we were able to associate the common single nucleotides polymorphism (SNP) rs2513192 with *TRPC6* expression in tibial arteries with the A-allele being associated with increased proliferation (Wierer et al., 2021). To test if there is an association between *TRPC6* genotype and in-stent restenosis after coronary stenting, we next analyzed a dataset of patients who previously underwent coronary stenting and had angiographic follow-up data available (n=3,068 individuals, n=4,279 lesions) (**Figure 7A**). Patient and procedural characteristics are illustrated in Table 9.

Table 9 Baseline and procedural characteristics of individuals with available rs2513192 genotype. To test a possible correlation of rs2513192 genotype and in-stent-restenosis we performed a genetic analysis, which included all individuals with angiographic follow-ups. ACC/AHA, American College of Cardiology/American Heart Association; CABG, coronary artery bypass graft; CAD, coronary artery disease; MI, myocardial infarction; (N)STEMI, (Non-)ST-elevation myocardial infarction; PCI, percutaneous coronary intervention. Reprinted by permission from Oxford University Press: Supplemental Table S3 from European Heart Journal 2021. 42(10):1773-1785 (Wierer et al. 2021), copyright © 2021

	GG/AG (n=3,895; 5,510 lesions)	AA (n=352; 518 lesions)	p-value
Baseline characteristics*			
Male gender, n (%)	2,717 (69.8)	253 (71.9)	0.41
Age, years	58.5±11.0	58.5±11.1	0.89
Body mass index, kg/m^2	27.6±4.4	27.3±4.5	0.24
Insulin-dependent diabetes mellitus, n (%)	283 (7.3)	23 (6.5)	0.61
Hypertension, n (%)	3,103 (79.7)	282 (80.1)	0.84
Hypercholesterolemia, n (%)	2,821 (72.4)	262 (74.4)	0.42
Smoker, n (%)	1,187 (30.5)	100 (28.4)	0.42
Positive family history, n (%)	1,832 (47.0)	161 (45.7)	0.64
Clinical presentation			0.42
STEMI, n (%)	816 (20.9)	64 (18.2)	
NSTEMI, n (%)	267 (6.9)	21 (6.0)	
Unstable angina, n (%)	651 (16.7)	56 (15.9)	
Stable CAD	2,161 (55.5)	211 (59.9)	
Previous MI, n (%)	1,715 (44.0)	161 (45.7)	0.54
Previous CABG, n (%)	342 (8.8)	35 (9.9)	0.46
Previous PCI, n (%)	2,033 (52.2)	189 (53.7)	0.59
Number of affected coronary vessels			0.58
1-vessel disease, n (%)	972 (25.0)	94 (26.7)	
2-vessel disease, n (%)	1,147 (29.4)	95 (27.0)	
3-vessel disease, n (%)	1,776 (45.6)	163 (46.3)	

Left ventricular ejection fraction, %	53.0±12.3	52.7±13.3	0.72
Procedural characteristics			
Multiple lesions, n (%)*	1,221 (31.3)	124 (35.2)	0.13
Affected vessel, n (%)†			
Left main, n (%)	159 (2.9)	14 (2.7)	0.94
Left anterior descending, n (%)	2,284 (41.5)	218 (42.1)	
Left circumflex, n (%)	1,359 (24.7)	122 (23.5)	
Right coronary artery, n (%)	1,708 (30.9)	164 (31.7)	
ACC/AHA type B2 or C, n (%)†	3,796 (68.9)	346 (66.8)	0.32
Complete occlusion, n (%)†	296 (5.4)	26 (5.0)	0.73
In-stent restenosis, n (%)†	674 (12.2)	70 (13.5)	0.40
Stent type†			
Bare metal stent, n (%)	2,047 (37.2)	131 (36.9)	0.96
1st Generation drug eluting stent, n (%)	1,225 (22.2)	118 (22.8)	
2nd Generation drug eluting stent, n (%)	2,238 (40.6)	209 (40.3)	
Lesion length, mm†	14.6±8.6	14.8±9.1	0.67
Stenosis before PCI, %†	66.8±18.5	66.9±19.2	0.90
Stenosis after PCI, %†	9.1±8.1	9.4±8.8	0.41
Nominal balloon diameter, mm†	3.1±0.6	3.2±0.6	0.24
Maximum balloon pressure, atm†	14.1±3.1	14.2±3.2	0.51
Total stented length, mm†	23.6±11.4	23.6±11.5	0.94
Angiographic follow-up*			
Angiographic follow-up available			
Patients, n (%)	2,800 (72.0)	257 (73.0)	0.67
Lesions, n (%)	3,910 (71.0)	369 (71.2)	0.9
Time to angiographic follow-up, days	216.6±156.4	222.9±162.5	0.55

Restenosis was defined as a lumen diameter reduction of 50 % or more (binary restenosis) and was detected in 65 of 369 AA (17.6 %), 230 of 1,761 AG (13.1 %) and 268 of 2,149 GG lesions (12.5 %) (**Figure 7B**). On patient-level, restenosis was detected in 223 of 1,561 GG (14.3 %), 202 of 1,250 AG (16.2 %) and 56 of 257 AA patients (21.8 %) (**Figure 7C**). The A-allele was associated with an increased risk of binary restenosis with an OR of 1.46 [95 % CI 1.08 - 1.95] and a significant gene-dosage effect (GG 12.5 vs. AG 13.1 vs. 17.6 %, p =0.03). A multivariate analysis of patients, who underwent coronary stenting, demonstrated that the A-allele remained a strong predictor of binary restenosis with an OR of 1.49 [95 % CI 1.08 – 2.05] (**Table 10**).

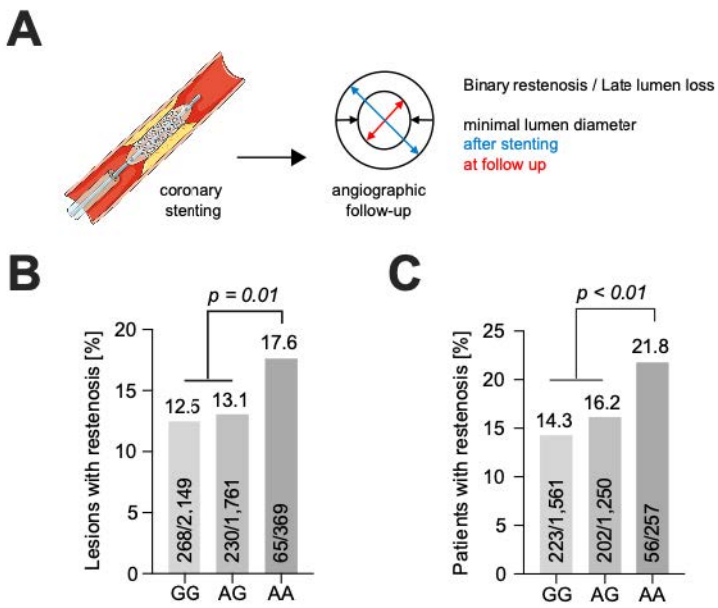

Figure 7: Angiographic follow-up analysis and the risk of restenosis after coronary stenting **A**, Angiographic follow-up analysis after coronary stenting **B**, Homozygous A-allele carriers (AA) vs. homozygous/heterozygous (GG/AG) G-Allele carriers and their respective risk of developing restenosis in lesions after coronary stenting **C**, Homozygous A-allele carriers (AA) vs. homozygous/heterozygous (GG/AG) G-Allele carriers and their respective risk of developing restenosis in a patient collective after coronary stenting. Data are in per cent. Reprinted by permission from Oxford University Press: Figure 7 D-F from European Heart Journal 2021. 42(10):1773-1785 (Wierer et al. 2021), copyright © 2021

Table 10 Multivariate analysis of rs2513192 AA genotype with in-stent restenosis after PCI with stent implantation. To build a model that avoids overfitting we considered the selection of covariates in the logistic regression. For this purpose, we used the least absolute shrinkage and selection operator regression method after entering all baseline and procedural characteristics as candidates (Table 9). ACC/AHA, American College of Cardiology/American Heart Association; CABG, coronary artery bypass graft; ACS, acute coronary syndrome; MI, myocardial infarction; BMI, body mass index; PCI, percutaneous coronary intervention. Reprinted by permission from Oxford University Press: Supplemental Table S4 from European Heart Journal 2021. 42(10):1773-1785 (Wierer et al. 2021), copyright © 2021

Covariate	Odds Ratio [95% Confidence Interval]	p-value
Homozygous AA genotype	1.49 [1.08-2.05]	0.01
Age	0.93 [0.8-1.08]	0.34
Male gender	1.31 [1.04-1.64]	0.02
BMI	1.02 [0.9-1.16]	0.78
Diabetes	1.61 [1.27-2.03]	<0.001
Hypertension	1.04 [0.8-1.36]	0.76
Smoking	0.95 [0.75-1.19]	0.64
Hypercholesterolemia	1.39 [1.09-1.77]	0.01
Previous MI	1.11 [0.89-1.38]	0.36
Previous CABG	1.53 [1.13-2.07]	0.01
Presentation with ACS	1.02 [0.82-1.27]	0.86
Multivessel disease	0.91 [0.71-1.17]	0.48
ACC/AHA complex lesion	1.34 [1.06-1.68]	0.01
Chronic occlusion	0.99 [0.64-1.52]	0.97
In-stent restenosis	2.67 [2.01-3.55]	<0.0001
Lesion length	0.96 [0.84-1.10]	0.57
Reference diameter before PCI	0.56 [0.48-0.65]	<0.0001
Stenosis grade before PCI	1.33 [1.16-1.53]	<0.0001
Drug eluting stent	0.18 [0.15-0.23]	<0.0001
Total stented length	1.41 [1.25-1.59]	<0.0001

5 Discussion

PCI is nowadays the preferred revascularization approach to treat CAD, which mainly arise as a consequence of atherosclerosis (Byrne et al., 2017). However, harmful vascular remodeling remains a serious concern and a major limitation following PCI. Balloon dilatation of narrowed vessels and stent placement forms a scar tissue, which can lead to intimal hyperplasia (Newby and Zaltsman, 2000). The responsible factors contributing to intimal hyperplasia were shown to be influenced by an accumulation of VSMC, ECM and inflammatory cells (Welt Frederick & Rogers, 2002). Intimal hyperplasia on its own can lead to re-narrowing of the stented segment, defined as restenosis, which is associated with morbidity and mortality (Cassese et al., 2014). For that, investigating different pathways leading to restenosis and finding possible future molecular targets to prevent the process of neointima formation is of outmost importance in the field of cardiovascular research.

Due to the high degree of difficulty in collecting human samples, the mouse has been the animal of choice to investigate different human disease in a standardized manner (Hui, 2008). Since stent implantation is not yet feasible in mice, our group induced wire injury of the left femoral artery of the C57BL/6J mice strain to study the process of neointima formation on a proteomic level. A drastic tissue remodeling was observed with the most prominent changes affecting ECM, immune response and migration pathways. Furthermore by using time-resolved proteomics, we were able to identify and characterize proteins with an early, late or transient regulation in response to vascular injury and observed that more than a half of them were either up- or downregulated at day three after injury (Wierer et al., 2021).

In this study, we were especially interested in highly expressed proteins at an early timepoint as these could drive the onset of neointima formation and hence be a possible pharmacological target to prevent restenosis. With this aim, we performed a pairwise comparison at days three and 14 on significantly upregulated proteins related to migration pathways of injured and non-injured vessels and identified among others the calcium ion channel Trpc6 to be predominantly upregulated at day three after injury (Wierer et al., 2021). We chose Trpc6 for further validation as a promising molecular target that could be involved in the neointima formation considering its expression pattern in injured and non-injured vessels [for details see (Wierer et al., 2021)] and its

previous association with cell migration in breast cancer cells (Jardin et al., 2018) and leukocyte transendothelial migration during inflammatory response (Weber et al., 2015).

TRPC6 is part of the canonical TRP-channel family. The non-selective cation channel is six fold more permeable to Ca^{2+} than Na^{+} (Dietrich et al., 2003; Hofmann et al., 1999; Shi et al., 2004) and is activated by DAG following ($PI(4,5)P_2$) hydrolysis by surface receptor-coupled PLC (Hofmann et al., 1999). The full functionality of TRPC6 is assumed to be accredited to their homo- and heterotetrametric complexes formation at the plasma membrane (Dietrich et al., 2003). The exact physiological role of TRPC6 is still unknown, but a biological relevance of TRPC6 has been shown in immune and blood cells, tumor development, in neural function and in the kidney [reviewed in (Dietrich & Gudermann, 2014)]. In VSMC, TRPC6 was shown to be an essential component of α_1-adrenoreceptors (Inoue et al., 2001) and its upregulation was found to stimulate PDGF-induced SMC proliferation (Yu et al., 2003).

We first aimed to validate the upregulation of Trpc6 and analyzed injured and non-injured femoral arteries of the C57BL/6J mice regarding Trpc6 expression after three, seven and 14 days using an independent method. In Western Blot analyses, we confirmed a strong increase in Trpc6 protein levels early after injury with subsequently decreasing signal intensities. While this result confirms that more Trpc6 is available in the early phase after injury, the underlying mechanism remains unknown and will be subject for follow-up projects to better understand the role of TRPC6 in vascular injury.

The first question in this study sought to determine the downstream cellular consequences of altered TRPC6 availability. Little is known about the molecular activators that triggers phenotypic changes to VSMC, which is the basis of VSMC migration and proliferation involved in restenosis and neointima formation after vascular injury (Newby & Zaltsman, 2000; Rensen et al., 2007). For that, we investigated the effect of TRPC6 on VSMC proliferation/migration *in vitro* by modulating its activity using activators and inhibitors. By performing migration wound scratch and proliferation assays *in vitro*, we found out that the TRPC6 activator OAG enhanced VSMC migration and proliferation. In line, the TRPC6 inhibitor SAR7334 (Maier et al., 2015) was found to reduce VSMC migration in migration scratch wound assays. These results match those observed in earlier studies (Numaga-Tomita et al., 2019) and it therefore support our hypothesis that particularly TRPC6 in VSMC might play a role in neointima formation. However, further research is required to determine the effects of modulating

TRPC6 activity on ECM remodeling as this can also be implicated in the process of neointima formation.

To test a possible clinical application, we further performed radius migration assays with SAR7334 coated dishes. Results of these analyses were consistent with the results obtained in migration scratch wound assays and revealed that SAR7334 led to decreased VSMC migration *in vitro*. Taken together, coating surfaces with a TRPC6 inhibitor seems feasible to reduce VSMC migration.

To prove that TRPC6 plays a causal role in neointima formation, it was, however, necessary to study the phenotype in mice lacking Trpc6, the murine counterpart. Indeed, we found that lack of Trpc6 reduced neointima formation secondary to wire-injury supporting a pivotal role of Trpc6 in vascular pathophysiology. In accordance with the present results, previous studies have demonstrated that PDGF receptor kinase inhibitors reduce neointima formation [reviewed in (Levitzki, 2005)]. However, it remains unclear to which degree the increased TRPC6 expression is attributed only to VSMC. Further research should be undertaken to investigate the TRPC6 expression from other cell types such as fibroblasts and endothelial cells, which can also contribute in the mechanism.

Our understanding of different biological pathways leading to a specific human disease and the later drug development has been greatly improved by studies derived from mouse models (Von Scheidt et al., 2017). However, the efficacy of treatments described in animal models could not always be translated in human clinical trials (Mak et al., 2014). To test the consistency of the *in vivo* results in humans, we aimed to compare our findings with genetic variants results from recent GWAS. Erdmann et al. associated 163 genetic loci with an increased risk of CAD or MI (Erdmann et al., 2018). It is interesting to note that the *TRPC6* locus was not identified to generate a suggestive signal for CAD (Erdmann et al., 2018). However, by querying the GTEX dataset (Consortium, 2013) we were able to identify a common SNP that is associated with *TRPC6* expression in tibial arteries. Interestingly, the allele which is associated with highest *TRPC6* expression was also associated with increased proliferation capacity of VSMC mediated by PDGF. Overall, this finding supports the *in vitro* findings and indicate a TRPC6 implication in vascular remodeling.

Finally, we aimed at investigating whether *TRPC6* genotype is associated with restenosis after coronary stenting. Patients, with genetically augmented *TRPC6*

expression were found to have a 59 % higher restenosis risk. This finding suggests that *TRPC6* expression can be used as an indicator to identify patients with a higher risk of restenosis. However, in addition to the *in vitro* and *in vivo* findings, the most obvious finding to merge from the genetic analyses is that TRPC6 might be involved in neointima formation and vascular remodeling, representing a possible novel target to treat restenosis after vascular injury.

As discussed above, increased PDGF expression is widely believed to be the main driver of the early process of neointima formation due to its promigratory and proliferative effect to VSMC. Its binding to the PDGF-receptor activates different downstream signaling pathways which raise intracellular Ca^{2+} concentration and TRPC6-mediated calcium entry is believed to contribute (Bisaillon et al., 2010; Jia et al., 2017). Among others, PLC and PI3K/AKT/mammalian target of rapamycin (mTOR) signal transduction pathway are activated (Shaw & Cantley, 2006). mTOR acts as a critical growth-node for VSMC by stimulating downstream the p70 S6 kinase, which leads to increased synthesis of cell cycle proteins and subsequently increased migration and proliferation of VSMC (Shaw & Cantley, 2006). The PI3K signal transduction pathway has been the target of antiproliferative agents used as coated drugs in DES, as it was shown that PI3K/Akt activation is negatively regulated by mTOR (Zhang et al., 2007). DES are nowadays the preferred stent type used in revascularization as studies such as that conducted by Kastrati et al. (2007) have shown that they can significantly reduce restenosis and the need for revascularization compared to previously used BMS (Kastrati et al., 2007).

As described above, PDGF-mediated VSMC proliferation following PLC activation was associated with high TRPC6 expression in tibial arteries and this pathway seems to be independent of mTOR signaling. Moreover, in *vitro* and in *vivo* experiments showed a possible TRPC6 implication in the neointima formation. These findings suggest that inhibition of TRPC6 could prevent restenosis following coronary stenting. Hence, it could conceivably be hypothesized that inhibition of TRPC6 could represent an alternative or complementary way to routinely used mTOR inhibitors which can lead to a further reduction of neointima formation and subsequently restenosis risk (**Figure 8**).

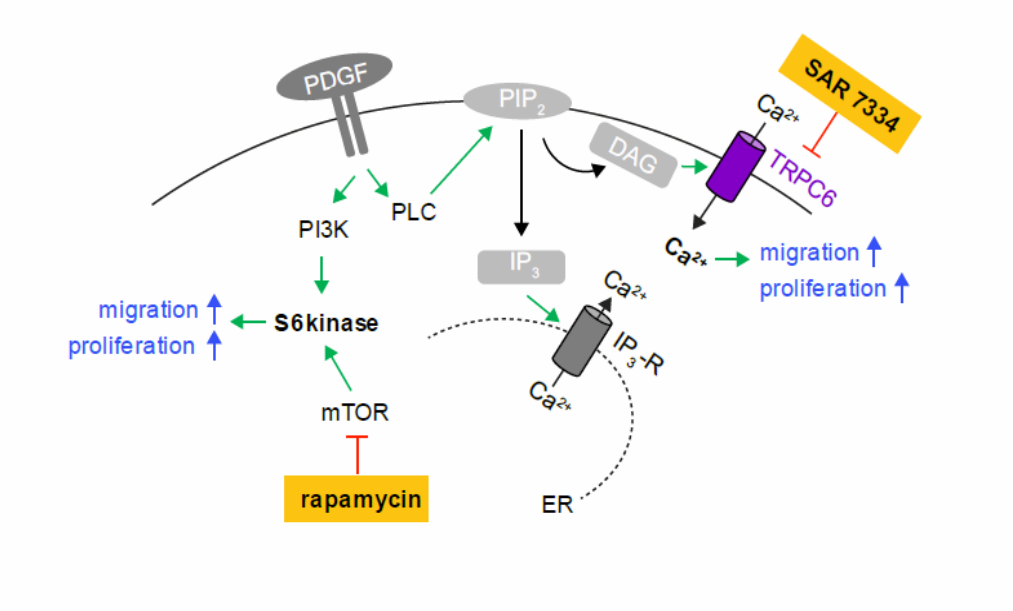

Figure 8: TRPC6 inhibition as a complementary pathway to reduce neointima formation PI3K, Phosphatidylinositol-3-kinase: PLC, phospholipase C: PIP2, phosphatidylinositol-4,5-bisphosphate: IP3, phosphatidylinositol-3,4,5-trisphosphate: DAG, Diaycylglycerol: IP_3R, phosphatidylinositol-3,4,5-triphosphate-receptor: ER. Endoplasmatic reticulum: mTOR, mammalian target of rapamycin: Following binding of PDGF to the PDGF receptor, the PI3K signaling pathway and PLC are activated. PI3K downstream substrate is mTOR, which stimulates S6 protein kinase to increase migration and proliferation capacity of VSMC. Rapamycin inhibits this pathway and hence reduces the neointima formation. PLC cleaves the membrane-bound PIP2 to generate DAG and IP_3. IP_3 binds to the IP_3R receptor of ER and can raise the cytosolic Ca^{2+} concentration. DAG activates TRPC6 channel, which in this study was shown to lead to increased migration and proliferation of VSMC. The TRPC6 Inhibitor, SAR7334, inhibits TRPC6 CA^{2+} influx and leads to reduced migration and proliferation and subsequently reduces neointima formation and restenosis risk. Reprinted by permission from Oxford University Press: Study scheme and hypothesis from European Heart Journal 2021. 42(10):1773-1785 (Wierer et al. 2021), copyright © 2021

Since an involvement of TRPC6 was shown in pathological conditions such as FSGS, lung fibrosis and cardiac hypertrophy and its exact physiological role is still not completely clear [reviewed in (Dietrich & Gudermann, 2014)], we hypothesize that inhibitors of TRPC6 could therefore be much safer than in DES routinely used mTOR inhibitors. To conclude, TRPC6 could be a novel drug target especially in the early phase after stent implantation and a novel therapeutic option for a certain group of patients. However, we cannot rule out that other ion channels, transporters or Ca^{2+} signaling molecules could be involved in the mechanisms. The exact role of TRPC6 still needs to be elucidated and therefore further research is needed.

6 Summary

Neointima formation and restenosis remain a serious concern associated with mortality and morbidity following percutaneous coronary intervention (PCI) and stent implantation. Therefore, unraveling the mechanism leading to neointima formation is of outmost importance in the field of cardiovascular research. Vascular smooth muscle cells (VSMC) proliferation and migration are hallmarks of neointima formation. For that, capacitative calcium (Ca^{2+}) entry and changes in cytosolic free Ca^{2+} concentration are required. Using deep proteomic profiling of injured murine femoral arteries, our research group identified canonical transient receptor channel six (Trpc6) to be upregulated in the early phase after vascular injury, i.e., Trpc6 was transiently upregulated. TRPC6 is a Ca^{2+} permeable non-selective cation channel, which is believed to operate as a receptor operated channel and was previously associated with migration in breast cancer cell lines and leukocyte transendothelial migration. So far, however, the role of TRPC6 in VSMC remains unknown. This dissertation set out to investigate the role of TRPC6 in neointima formation following vascular injury with the hope of finding new targets for therapeutic treatments. To assess whether TRPC6 effects proliferation and migration of VSMC in *vitro*, we performed migration scratch and proliferation assays after modulating TRPC6 activity. We found that the TRPC6 activator 1-Oleoyl-2-acetyl-sn-glycerol (OAG) led to increased migration and proliferation. In line with this, we observed a reduced migration of VSMC after treatment with the TRPC6 inhibitor SAR7334. Moreover, we employed a knockout mouse model to investigate the consequence of Trpc6 silencing *in vivo*. A pairwise comparison of $Trpc6^{-/-}$ mice with wild-type mice at 28 days after vascular injury revealed a reduced neointima formation in $Trpc6^{-/-}$ mice. Finally, we asked if genetically expressed *TRPC6* expression could influence the risk of restenosis after coronary stenting. For that, we analyzed angiographic follow-up data of individuals who previously underwent PCI and coronary stenting. We identified that genetically augmented *TRPC6* expression was associated with a significant higher restenosis risk. In this study, we present TRPC6 as a future possible drug target to reduce the burden of neointima formation following vascular injury and stent implantation.

7 Bibliography

Aslam, B., Basit, M., Nisar, M. A., Khurshid, M., & Rasool, M. H. (2017). Proteomics: Technologies and Their Applications. *Journal of Chromatographic Science*, *55*(2), 182-196. https://doi.org/10.1093/chromsci/bmw167

Bendeck, M. P., Zempo, N., Clowes, A. W., Galardy, R. E., & Reidy, M. A. (1994). Smooth muscle cell migration and matrix metalloproteinase expression after arterial injury in the rat. *Circulation Research*, *75*(3), 539-545. https://doi.org/10.1161/01.RES.75.3.539

Benjamin, E. J., Virani, S. S., Callaway, C. W., Chamberlain, A. M., Chang, A. R., Cheng, S., . . . Muntner, P. (2018). Heart Disease and Stroke Statistics—2018 Update: A Report From the American Heart Association. *Circulation*, *137*(12), CIR.00000000000. https://doi.org/10.1161/cir.0000000000000558

Berridge, M. J. (1995). Calcium signalling and cell proliferation. *BioEssays*, *17*(6), 491-500. https://doi.org/10.1002/bies.950170605

Berridge, M. J. (2012). Calcium signalling remodelling and disease. *Biochem Soc Trans*, *40*(2), 297-309. https://doi.org/10.1042/bst20110766

Bisaillon, J. M., Motiani, R. K., Gonzalez-Cobos, J. C., Potier, M., Halligan, K. E., Alzawahra, W. F., . . . Trebak, M. (2010). Essential role for STIM1/Orai1-mediated calcium influx in PDGF-induced smooth muscle migration. *American journal of physiology. Cell physiology*, *298*(5), C993-C1005. https://doi.org/10.1152/ajpcell.00325.2009

Blanc-Brude, O. P., Yu, J., Simosa, H., Conte, M. S., Sessa, W. C., & Altieri, D. C. (2002). Inhibitor of apoptosis protein survivin regulates vascular injury. *Nature Medicine*, *8*(9), 987-994. https://doi.org/10.1038/nm750

Boccardi, C., Cecchettini, A., Caselli, A., Camici, G., Evangelista, M., Mercatanti, A., . . . Citti, L. (2007). A proteomic approach to the investigation of early events involved in vascular smooth muscle cell activation. *Cell and Tissue Research*, *328*(1), 185-195. https://doi.org/10.1007/s00441-006-0357-3

Bonnans, C., Chou, J., & Werb, Z. (2014). Remodelling the extracellular matrix in development and disease. *Nature Reviews Molecular Cell Biology*, *15*(12), 786-801. https://doi.org/10.1038/nrm3904

Buccheri, D., Piraino, D., Andolina, G., & Cortese, B. (2016). Understanding and managing in-stent restenosis: a review of clinical data, from pathogenesis to treatment. *Journal of Thoracic Disease*, *8*(10), E1150-E1162. https://doi.org/10.21037/jtd.2016.10.93

Byrne, R. A., Stone, G. W., Ormiston, J., & Kastrati, A. (2017). Coronary balloon angioplasty, stents, and scaffolds. *The Lancet*, *390*(10096), 781-792. https://doi.org/10.1016/s0140-6736(17)31927-x

Cassese, S., Byrne, R. A., Ndrepepa, G., Schunkert, H., Fusaro, M., & Kastrati, A. (2015). Prolonged dual antiplatelet therapy after drug-eluting stenting: meta-analysis of randomized trials. *Clin Res Cardiol*, *104*(10), 887-901. https://doi.org/10.1007/s00392-015-0860-1

Cassese, S., Byrne, R. A., Schulz, S., Hoppman, P., Kreutzer, J., Feuchtenberger, A., . . . Kastrati, A. (2014). Prognostic role of restenosis in 10 004 patients undergoing routine control angiography after coronary stenting. *European Heart Journal*, *36*(2), 94-99. https://doi.org/10.1093/eurheartj/ehu383

Chistiakov, D. A., Sobenin, I. A., & Orekhov, A. N. (2013). Vascular extracellular matrix in atherosclerosis. *Cardiol Rev*, *21*(6), 270-288. https://doi.org/10.1097/CRD.0b013e31828c5ced

Chung, I.-M. O., Gold, H. K., Schwartz, S. M., Ikari, Y., Reidy, M. A., & Wight, T. N. (2002). Enhanced extracellular matrix accumulation in restenosis of coronary arteries after stent deployment. *Journal of the American College of Cardiology*, *40*(12), 2072-2081. https://doi.org/10.1016/s0735-1097(02)02598-6

Clapham, D. E. (1995). Calcium signaling. *Cell*, *80*(2), 259-268. https://doi.org/10.1016/0092-8674(95)90408-5

Clapham, D. E., Runnels, L. W., & Strübing, C. (2001). The trp ion channel family. *Nature Reviews Neuroscience*, *2*(6), 387-396. https://doi.org/10.1038/35077544

Clowes, A. W., Reidy, M. A., & Clowes, M. M. (1983). Mechanisms of stenosis after arterial injury. *Lab Invest*, *49*(2), 208-215.

Cohn, W. E. (2010). Advances in surgical treatment of acute and chronic coronary artery disease. *Texas Heart Institute journal*, *37*(3), 328-330. https://pubmed.ncbi.nlm.nih.gov/20548814
https://www.ncbi.nlm.nih.gov/pmc/articles/PMC2879187/

Consortium, G. T. (2013). The Genotype-Tissue Expression (GTEx) project. *Nature Genetics*, *45*(6), 580-585. https://doi.org/10.1038/ng.2653

Cutlip, D. E., Windecker, S., Mehran, R., Boam, A., Cohen, D. J., Van Es, G.-A., . . . Serruys, P. W. (2007). Clinical End Points in Coronary Stent Trials. *Circulation*, *115*(17), 2344-2351. https://doi.org/10.1161/circulationaha.106.685313

de la Cuesta, F., Alvarez-Llamas, G., Gil-Dones, F., Darde, V. M., Calvo, E., López, J. A., . . . Barderas, M. G. (2013). Secretome of Human Aortic Valves. In F. Vivanco (Ed.), *Heart Proteomics: Methods and Protocols* (pp. 237-243). Humana Press. https://doi.org/10.1007/978-1-62703-386-2_19

Deb, S., Wijeysundera, H. C., Ko, D. T., Tsubota, H., Hill, S., & Fremes, S. E. (2013). Coronary Artery Bypass Graft Surgery vs Percutaneous Interventions in Coronary Revascularization. *JAMA*, *310*(19), 2086. https://doi.org/10.1001/jama.2013.281718

Deracinois, B., Flahaut, C., Duban-Deweer, S., & Karamanos, Y. (2013). Comparative and Quantitative Global Proteomics Approaches: An Overview. *Proteomes*, *1*(3), 180-218. https://doi.org/10.3390/proteomes1030180

Dietrich, A., Chubanov, V., & Gudermann, T. (2010). Renal TRPathies. *Journal of the American Society of Nephrology*, *21*(5), 736-744. https://doi.org/10.1681/asn.2009090948

Dietrich, A., & Gudermann, T. (2007). Trpc6. *Handb Exp Pharmacol*(179), 125-141. https://doi.org/10.1007/978-3-540-34891-7_7

Dietrich, A., & Gudermann, T. (2014). TRPC6: Physiological Function and Pathophysiological Relevance. In B. Nilius & V. Flockerzi (Eds.), *Mammalian Transient Receptor Potential (TRP) Cation Channels: Volume I* (pp. 157-188). Springer Berlin Heidelberg. https://doi.org/10.1007/978-3-642-54215-2_7

Dietrich, A., Mederos y Schnitzler, M., Emmel, J., Kalwa, H., Hofmann, T., & Gudermann, T. (2003). N-linked protein glycosylation is a major determinant for basal TRPC3 and TRPC6 channel activity. *J Biol Chem*, *278*(48), 47842-47852. https://doi.org/10.1074/jbc.M302983200

Dietrich, A., Mederos, Y. S. M., Gollasch, M., Gross, V., Storch, U., Dubrovska, G., . . . Birnbaumer, L. (2005). Increased vascular smooth muscle contractility in TRPC6-/- mice. *Mol Cell Biol*, *25*(16), 6980-6989. https://doi.org/10.1128/MCB.25.16.6980-6989.2005

Dryer, S. E., & Reiser, J. (2010). TRPC6 channels and their binding partners in podocytes: role in glomerular filtration and pathophysiology. *Am J Physiol Renal Physiol*, *299*(4), F689-701. https://doi.org/10.1152/ajprenal.00298.2010

Du, W., Huang, J., Yao, H., Zhou, K., Duan, B., & Wang, Y. (2010). Inhibition of TRPC6 degradation suppresses ischemic brain damage in rats. *The Journal of Clinical Investigation*, *120*(10), 3480-3492. https://doi.org/10.1172/JCI43165

Dzau, V. J., Antman, E. M., Black, H. R., Hayes, D. L., Manson, J. E., Plutzky, J., . . . Stevenson, W. (2006). The Cardiovascular Disease Continuum Validated: Clinical Evidence of Improved Patient Outcomes. *Circulation*, *114*(25), 2850-2870. https://doi.org/doi:10.1161/CIRCULATIONAHA.106.655688

Erdmann, J., Kessler, T., Munoz Venegas, L., & Schunkert, H. (2018). A decade of genome-wide association studies for coronary artery disease: the challenges ahead. *Cardiovascular Research*, *114*(9), 1241-1257. https://doi.org/10.1093/cvr/cvy084

Forough, R., Koyama, N., Hasenstab, D., Lea, H., Clowes, M., Nikkari Seppo, T., & Clowes Alexander, W. (1996). Overexpression of Tissue Inhibitor of Matrix Metalloproteinase-1 Inhibits Vascular Smooth Muscle Cell Functions In Vitro and In Vivo. *Circulation Research*, *79*(4), 812-820. https://doi.org/10.1161/01.RES.79.4.812

Frangogiannis, N. G. (2017). The extracellular matrix in myocardial injury, repair, and remodeling. *Journal of Clinical Investigation*, *127*(5), 1600-1612. https://doi.org/10.1172/jci87491

Galis, Z. S., & Khatri, J. J. (2002). Matrix metalloproteinases in vascular remodeling and atherogenesis: the good, the bad, and the ugly. *Circ Res*, *90*(3), 251-262.

Graves, P. R., & Haystead, T. A. J. (2002). Molecular biologist's guide to proteomics. *Microbiology and molecular biology reviews : MMBR*, *66*(1), 39-63. https://doi.org/10.1128/mmbr.66.1.39-63.2002

Grüntzig, A. (1978). TRANSLUMINAL DILATATION OF CORONARY-ARTERY STENOSIS. *The Lancet*, *311*(8058), 263. https://doi.org/10.1016/s0140-6736(78)90500-7

Hansson, G. K. (2005). Inflammation, Atherosclerosis, and Coronary Artery Disease. *New England Journal of Medicine*, *352*(16), 1685-1695. https://doi.org/10.1056/nejmra043430

Hao, P., Ren, Y., Pasterkamp, G., Moll, F. L., de Kleijn, D. P., & Sze, S. K. (2014). Deep proteomic profiling of human carotid atherosclerotic plaques using multidimensional LC-MS/MS. *Proteomics. Clinical applications*, *8*(7-8), 631-635. https://doi.org/10.1002/prca.201400007

Heidenreich, P. A., Trogdon, J. G., Khavjou, O. A., Butler, J., Dracup, K., Ezekowitz, M. D., . . . Woo, Y. J. (2011). Forecasting the Future of Cardiovascular Disease in the United States. *Circulation*, *123*(8), 933-944. https://doi.org/doi:10.1161/CIR.0b013e31820a55f5

Hofmann, K., Fiedler, S., Vierkotten, S., Weber, J., Klee, S., Jia, J., . . . Dietrich, A. (2017). Classical transient receptor potential 6 (TRPC6) channels support myofibroblast differentiation and development of experimental pulmonary fibrosis. *Biochim Biophys Acta Mol Basis Dis*, *1863*(2), 560-568. https://doi.org/10.1016/j.bbadis.2016.12.002

Hofmann, T., Obukhov, A. G., Schaefer, M., Harteneck, C., Gudermann, T., & Schultz, G. (1999). Direct activation of human TRPC6 and TRPC3 channels by diacylglycerol. *Nature*, *397*(6716), 259-263. https://doi.org/10.1038/16711

House, S. J., Potier, M., Bisaillon, J., Singer, H. A., & Trebak, M. (2008). The non-excitable smooth muscle: Calcium signaling and phenotypic switching during vascular disease. *Pflügers Archiv - European Journal of Physiology*, *456*(5), 769-785. https://doi.org/10.1007/s00424-008-0491-8

Hui, D. Y. (2008). Intimal hyperplasia in murine models. *Current drug targets*, *9*(3), 251-260. https://doi.org/10.2174/138945008783755601

Inoue, R., Okada, T., Onoue, H., Hara, Y., Shimizu, S., Naitoh, S., . . . Mori, Y. (2001). The Transient Receptor Potential Protein Homologue TRP6 Is the Essential Component of Vascular α 1 -Adrenoceptor–Activated Ca 2+ -Permeable Cation Channel. *Circulation Research*, *88*(3), 325-332. https://doi.org/10.1161/01.res.88.3.325

Jardin, I., Diez-Bello, R., Lopez, J. J., Redondo, P. C., Salido, G. M., Smani, T., & Rosado, J. A. (2018). TRPC6 Channels Are Required for Proliferation, Migration and Invasion of Breast Cancer Cell Lines by Modulation of Orai1 and Orai3 Surface Exposure. *Cancers (Basel)*, *10*(9). https://doi.org/10.3390/cancers10090331

Jia, S., Rodriguez, M., Williams, A. G., & Yuan, J. P. (2017). Homer binds to Orai1 and TRPC channels in the neointima and regulates vascular smooth muscle cell migration and proliferation. *Scientific Reports*, *7*(1), 5075. https://doi.org/10.1038/s41598-017-04747-w

Joner, M., Finn, A. V., Farb, A., Mont, E. K., Kolodgie, F. D., Ladich, E., . . . Virmani, R. (2006). Pathology of Drug-Eluting Stents in Humans. *Journal of the American College of Cardiology*, *48*(1), 193-202. https://doi.org/10.1016/j.jacc.2006.03.042

Jukema, J. W., Ahmed, T. A. N., Verschuren, J. J. W., & Quax, P. H. A. (2012). Restenosis after PCI. Part 2: prevention and therapy. *Nature Reviews Cardiology*, *9*(2), 79-90. https://doi.org/10.1038/nrcardio.2011.148

Jung, S., Strotmann, R., Schultz, G., & Plant, T. D. (2002). TRPC6 is a candidate channel involved in receptor-stimulated cation currents in A7r5 smooth muscle cells. *Am J Physiol Cell Physiol*, *282*(2), C347-359. https://doi.org/10.1152/ajpcell.00283.2001

Kang, D. H., Choi, M., Chang, S., Lee, M. Y., Lee, D. J., Choi, K., . . . Kang, S. W. (2015). Vascular Proteomics Reveal Novel Proteins Involved in SMC Phenotypic Change: OLR1 as a SMC Receptor Regulating Proliferation and Inflammatory Response. *PLoS One*, *10*(8), e0133845. https://doi.org/10.1371/journal.pone.0133845

Kastrati, A., Mehilli, J., Dirschinger, J., Dotzer, F., SchüHlen, H., Neumann, F.-J., . . . SchöMig, A. (2001). Intracoronary Stenting and Angiographic Results. *Circulation*, *103*(23), 2816-2821. https://doi.org/10.1161/01.cir.103.23.2816

Kastrati, A., Mehilli, J., Pache, J., Kaiser, C., Valgimigli, M., Kelbæk, H., . . . Schömig, A. (2007). Analysis of 14 Trials Comparing Sirolimus-Eluting Stents with Bare-Metal Stents. *New England Journal of Medicine*, *356*(10), 1030-1039. https://doi.org/10.1056/nejmoa067484

Kessler, T., Erdmann, J., & Schunkert, H. (2013). Genetics of coronary artery disease and myocardial infarction--2013. *Curr Cardiol Rep*, *15*(6), 368. https://doi.org/10.1007/s11886-013-0368-0

Kessler, T., Vilne, B., & Schunkert, H. (2016). The impact of genome-wide association studies on the pathophysiology and therapy of cardiovascular disease. *EMBO Molecular Medicine*, *8*(7), 688-701. https://doi.org/10.15252/emmm.201506174

Kim, M. S., & Dean, L. S. (2011). In-Stent Restenosis. *Cardiovascular Therapeutics*, *29*(3), 190-198. https://doi.org/10.1111/j.1755-5922.2010.00155.x

Knuuti, J., Wijns, W., Saraste, A., Capodanno, D., Barbato, E., Funck-Brentano, C., . . . Group, E. S. D. (2019). 2019 ESC Guidelines for the diagnosis and management of chronic coronary syndromes: The Task Force for the diagnosis and management of chronic coronary syndromes of the European Society of Cardiology (ESC). *European Heart Journal*, *41*(3), 407-477. https://doi.org/10.1093/eurheartj/ehz425

Kulik, A. (2017). Quality of life after coronary artery bypass graft surgery versus percutaneous coronary intervention: what do the trials tell us? *Curr Opin Cardiol*, *32*(6), 707-714. https://doi.org/10.1097/hco.0000000000000458

Kuwahara, K., Wang, Y., McAnally, J., Richardson, J. A., Bassel-Duby, R., Hill, J. A., & Olson, E. N. (2006). TRPC6 fulfills a calcineurin signaling circuit during pathologic cardiac remodeling. *J Clin Invest*, *116*(12), 3114-3126. https://doi.org/10.1172/JCI27702

Lee, A. R., Lamb, R. R., Chang, J. H., Erdmann-Gilmore, P., Lichti, C. F., Rohrs, H. W., . . . Culican, S. M. (2012). Identification of Potential Mediators of Retinotopic Mapping: A Comparative Proteomic Analysis of Optic Nerve from WT and Phr1 Retinal Knockout Mice. *Journal of Proteome Research*, *11*(11), 5515-5526. https://doi.org/10.1021/pr300767a

Lee, K., Forudi, F., Saidel, G. M., & Penn, M. S. (2005). Alterations in Internal Elastic Lamina Permeability As a Function of Age and Anatomical Site Precede Lesion Development in Apolipoprotein E–Null Mice. *Circulation Research*, *97*(5), 450-456. https://doi.org/doi:10.1161/01.RES.0000181026.94390.c9

Lee, M. S., David, E. M., Makkar, R. R., & Wilentz, J. R. (2004). Molecular and cellular basis of restenosis after percutaneous coronary intervention: the intertwining roles of platelets, leukocytes, and the coagulation–fibrinolysis system. *The Journal of Pathology*, *203*(4), 861-870. https://doi.org/10.1002/path.1598

Levitzki, A. (2005). PDGF receptor kinase inhibitors for the treatment of restenosis. *Cardiovascular Research*, *65*(3), 581-586. https://doi.org/10.1016/j.cardiores.2004.08.008

Libby, P. (2009). Molecular and cellular mechanisms of the thrombotic complications of atherosclerosis. *Journal of lipid research*, *50 Suppl*(Suppl), S352-S357. https://doi.org/10.1194/jlr.R800099-JLR200

Libby, P., Buring, J. E., Badimon, L., Hansson, G. K., Deanfield, J., Bittencourt, M. S., . . . Lewis, E. F. (2019). Atherosclerosis. *Nature Reviews Disease Primers*, *5*(1), 56. https://doi.org/10.1038/s41572-019-0106-z

Libby, P., Okamoto, Y., Rocha, V. Z., & Folco, E. (2010). Inflammation in Atherosclerosis. *Circulation Journal*, *74*(2), 213-220. https://doi.org/10.1253/circj.cj-09-0706

Libby, P., Ridker, P. M., & Hansson, G. K. (2011). Progress and challenges in translating the biology of atherosclerosis. *Nature*, *473*(7347), 317-325. https://doi.org/10.1038/nature10146

Lindemann, O., Umlauf, D., Frank, S., Schimmelpfennig, S., Bertrand, J., Pap, T., . . . Schwab, A. (2013). TRPC6 regulates CXCR2-mediated chemotaxis of murine neutrophils. *J Immunol*, *190*(11), 5496-5505. https://doi.org/10.4049/jimmunol.1201502

Lloyd-Jones, D. M., Larson, M. G., Beiser, A., & Levy, D. (1999). Lifetime risk of developing coronary heart disease. *The Lancet*, *353*(9147), 89-92. https://doi.org/10.1016/s0140-6736(98)10279-9

Lüscher, T. F., Steffel, J., Eberli, F. R., Joner, M., Nakazawa, G., Tanner, F. C., & Virmani, R. (2007). Drug-eluting stent and coronary thrombosis: biological mechanisms and clinical implications. *Circulation*, *115*(8), 1051-1058. https://doi.org/10.1161/circulationaha.106.675934

Lusis, A. J. (2000). Atherosclerosis. *Nature*, *407*(6801), 233-241. https://doi.org/10.1038/35025203

Mahmood, T., & Yang, P.-C. (2012). Western blot: technique, theory, and trouble shooting. *North American journal of medical sciences*, *4*(9), 429-434. https://doi.org/10.4103/1947-2714.100998

Maier, T., Follmann, M., Hessler, G., Kleemann, H. W., Hachtel, S., Fuchs, B., . . . Strübing, C. (2015). Discovery and pharmacological characterization of a novel potent inhibitor of diacylglycerol-sensitive TRPC cation channels. *British Journal of Pharmacology*, *172*(14), 3650-3660. https://doi.org/10.1111/bph.13151

Mak, I. W., Evaniew, N., & Ghert, M. (2014). Lost in translation: animal models and clinical trials in cancer treatment. *American journal of translational research*, *6*(2), 114-118. https://pubmed.ncbi.nlm.nih.gov/24489990 https://www.ncbi.nlm.nih.gov/pmc/articles/PMC3902221/

Mayer, B., Erdmann, J., & Schunkert, H. (2007). Genetics and heritability of coronary artery disease and myocardial infarction. *Clinical Research in Cardiology*, *96*(1), 1-7. https://doi.org/10.1007/s00392-006-0447-y

Mitra, A. K., Gangahar, D. M., & Agrawal, D. K. (2006). Cellular, molecular and immunological mechanisms in the pathophysiology of vein graft intimal hyperplasia. *Immunology and Cell Biology*, *84*(2), 115-124. https://doi.org/10.1111/j.1440-1711.2005.01407.x

Montell, C., Jones, K., Hafen, E., & Rubin, G. (1985). Rescue of the Drosophila phototransduction mutation trp by germline transformation. *Science*, *230*(4729), 1040-1043. https://doi.org/10.1126/science.3933112

Mori, M. X., Itsuki, K., Hase, H., Sawamura, S., Kurokawa, T., Mori, Y., & Inoue, R. (2015). Dynamics of receptor-operated Ca(2+) currents through TRPC channels controlled via the PI(4,5)P2-PLC signaling pathway. *Frontiers in pharmacology*, *6*, 22-22. https://doi.org/10.3389/fphar.2015.00022

Moses, J. W., Leon, M. B., Popma, J. J., Fitzgerald, P. J., Holmes, D. R., O'Shaughnessy, C., . . . Kuntz, R. E. (2003). Sirolimus-Eluting Stents versus Standard Stents in Patients with Stenosis in a Native Coronary Artery. *New England Journal of Medicine*, *349*(14), 1315-1323. https://doi.org/10.1056/NEJMoa035071

Nakazawa, G., Otsuka, F., Nakano, M., Vorpahl, M., Yazdani, S. K., Ladich, E., . . . Virmani, R. (2011). The Pathology of Neoatherosclerosis in Human Coronary Implants. *Journal of the American College of Cardiology*, *57*(11), 1314-1322. https://doi.org/10.1016/j.jacc.2011.01.011

Nesvizhskii, A. I., Vitek, O., & Aebersold, R. (2007). Analysis and validation of proteomic data generated by tandem mass spectrometry. *Nature Methods*, *4*(10), 787-797. https://doi.org/10.1038/nmeth1088

Neumann, F.-J., Sousa-Uva, M., Ahlsson, A., Alfonso, F., Banning, A. P., Benedetto, U., . . . Group, E. S. D. (2018). 2018 ESC/EACTS Guidelines on myocardial revascularization. *European Heart Journal*, *40*(2), 87-165. https://doi.org/10.1093/eurheartj/ehy394

Newby, A. C., & Zaltsman, A. B. (2000). Molecular mechanisms in intimal hyperplasia. *J Pathol*, *190*(3), 300-309. https://doi.org/10.1002/(SICI)1096-9896(200002)190:3<300::AID-PATH596>3.0.CO;2-I

Nilius, B., Owsianik, G., Voets, T., & Peters, J. A. (2007). Transient Receptor Potential Cation Channels in Disease. *Physiological Reviews*, *87*(1), 165-217. https://doi.org/10.1152/physrev.00021.2006

Numaga-Tomita, T., Shimauchi, T., Oda, S., Tanaka, T., Nishiyama, K., Nishimura, A., . . . Nishida, M. (2019). TRPC6 regulates phenotypic switching of vascular

smooth muscle cells through plasma membrane potential-dependent coupling with PTEN. *FASEB J*, *33*(9), 9785-9796. https://doi.org/10.1096/fj.201802811R

Pandey, A., & Mann, M. (2000). Proteomics to study genes and genomes. *Nature*, *405*(6788), 837-846. https://doi.org/10.1038/35015709

Peng, J., & Gygi, S. P. (2001). Proteomics: the move to mixtures. *Journal of Mass Spectrometry*, *36*(10), 1083-1091. https://doi.org/10.1002/jms.229

Rensen, S. S. M., Doevendans, P. A. F. M., & Van Eys, G. J. J. M. (2007). Regulation and characteristics of vascular smooth muscle cell phenotypic diversity. *Netherlands Heart Journal*, *15*(3), 100-108. https://doi.org/10.1007/bf03085963

Rhodin, J. (1980). Handbook of physiology: The cardiovascular system. *Architecture of the vessel wall*, 1-31.

Sata, M., Maejima, Y., Adachi, F., Fukino, K., Saiura, A., Sugiura, S., . . . Nagai, R. (2000). A Mouse Model of Vascular Injury that Induces Rapid Onset of Medial Cell Apoptosis Followed by Reproducible Neointimal Hyperplasia. *Journal of Molecular and Cellular Cardiology*, *32*(11), 2097-2104. https://doi.org/10.1006/jmcc.2000.1238

Schwartz, B. G., Economides, C., Mayeda, G. S., Burstein, S., & Kloner, R. A. (2010). The endothelial cell in health and disease: its function, dysfunction, measurement and therapy. *International Journal of Impotence Research*, *22*(2), 77-90. https://doi.org/10.1038/ijir.2009.59

Serruys, P. W., Morice, M.-C., Kappetein, A. P., Colombo, A., Holmes, D. R., Mack, M. J., . . . Mohr, F. W. (2009). Percutaneous Coronary Intervention versus Coronary-Artery Bypass Grafting for Severe Coronary Artery Disease. *New England Journal of Medicine*, *360*(10), 961-972. https://doi.org/10.1056/nejmoa0804626

Shaw, R. J., & Cantley, L. C. (2006). Ras, PI(3)K and mTOR signalling controls tumour cell growth. *Nature*, *441*(7092), 424-430. https://doi.org/10.1038/nature04869

Shen, X., Young, R., Canty, J. M., & Qu, J. (2014). Quantitative proteomics in cardiovascular research: global and targeted strategies. *Proteomics. Clinical applications*, *8*(7-8), 488-505. https://doi.org/10.1002/prca.201400014

Shi, J., Mori, E., Mori, Y., Mori, M., Li, J., Ito, Y., & Inoue, R. (2004). Multiple regulation by calcium of murine homologues of transient receptor potential proteins TRPC6 and TRPC7 expressed in HEK293 cells. *J Physiol*, *561*(Pt 2), 415-432. https://doi.org/10.1113/jphysiol.2004.075051

Stefanini, G. G., & Holmes, D. R. (2013). Drug-Eluting Coronary-Artery Stents. *New England Journal of Medicine*, *368*(3), 254-265. https://doi.org/10.1056/nejmra1210816

Tai, Y., Feng, S., Ge, R., Du, W., Zhang, X., He, Z., & Wang, Y. (2008). TRPC6 channels promote dendritic growth via the CaMKIV-CREB pathway. *J Cell Sci*, *121*(Pt 14), 2301-2307. https://doi.org/10.1242/jcs.026906

Tedgui, A., & Mallat, Z. (2006). Cytokines in Atherosclerosis: Pathogenic and Regulatory Pathways. *Physiological Reviews*, *86*(2), 515-581. https://doi.org/10.1152/physrev.00024.2005

Venter, J. C., Adams, M. D., Myers, E. W., Li, P. W., Mural, R. J., Sutton, G. G., . . . Zhu, X. (2001). The Sequence of the Human Genome. *Science*, *291*(5507), 1304-1351. https://doi.org/10.1126/science.1058040

Von Scheidt, M., Zhao, Y., Kurt, Z., Pan, C., Zeng, L., Yang, X., . . . Lusis, A. J. (2017). Applications and Limitations of Mouse Models for Understanding Human Atherosclerosis. *Cell Metabolism*, *25*(2), 248-261. https://doi.org/10.1016/j.cmet.2016.11.001

Wang, G. J., Sui, X. X., Simosa, H. F., Jain, M. K., Altieri, D. C., & Conte, M. S. (2005). Regulation of Vein Graft Hyperplasia by Survivin, an Inhibitor of Apoptosis Protein. *Arteriosclerosis, Thrombosis, and Vascular Biology*, *25*(10), 2081-2087. https://doi.org/10.1161/01.atv.0000183885.66153.8a

Weber, C., Zernecke, A., & Libby, P. (2008). The multifaceted contributions of leukocyte subsets to atherosclerosis: lessons from mouse models. *Nature Reviews Immunology*, *8*(10), 802-815. https://doi.org/10.1038/nri2415

Weber, E. W., Han, F., Tauseef, M., Birnbaumer, L., Mehta, D., & Muller, W. A. (2015). TRPC6 is the endothelial calcium channel that regulates leukocyte transendothelial migration during the inflammatory response. *The Journal of experimental medicine*, *212*(11), 1883-1899. https://doi.org/10.1084/jem.20150353

Welt Frederick, G. P., & Rogers, C. (2002). Inflammation and Restenosis in the Stent Era. *Arteriosclerosis, Thrombosis, and Vascular Biology*, *22*(11), 1769-1776. https://doi.org/10.1161/01.ATV.0000037100.44766.5B

Wierer, M., Werner, J., Wobst, J., Kastrati, A., Cepele, G., Aherrahrou, R., . . . Kessler, T. (2021). A proteomic atlas of the neointima identifies novel druggable targets for preventive therapy. *European Heart Journal*, *42*(18), 1773-1785. https://doi.org/10.1093/eurheartj/ehab140

Wilkins, M. R., Sanchez, J.-C., Gooley, A. A., Appel, R. D., Humphery-Smith, I., Hochstrasser, D. F., & Williams, K. L. (1996). Progress with Proteome Projects: Why all Proteins Expressed by a Genome Should be Identified and How To Do It. *Biotechnology and Genetic Engineering Reviews*, *13*(1), 19-50. https://doi.org/10.1080/02648725.1996.10647923

Xie, J., Cha, S. K., An, S. W., Kuro, O. M., Birnbaumer, L., & Huang, C. L. (2012). Cardioprotection by Klotho through downregulation of TRPC6 channels in the mouse heart. *Nat Commun*, *3*, 1238. https://doi.org/10.1038/ncomms2240

Yu, L.-R., Stewart, N. A., & Veenstra, T. D. (2010). Chapter 8 - Proteomics: The Deciphering of the Functional Genome. In G. S. Ginsburg & H. F. Willard (Eds.), *Essentials of Genomic and Personalized Medicine* (pp. 89-96). Academic Press. https://doi.org/https://doi.org/10.1016/B978-0-12-374934-5.00008-8

Yu, Y., Sweeney, M., Zhang, S., Platoshyn, O., Landsberg, J., Rothman, A., & Yuan, J. X. (2003). PDGF stimulates pulmonary vascular smooth muscle cell proliferation by upregulating TRPC6 expression. *Am J Physiol Cell Physiol*, *284*(2), C316-330. https://doi.org/10.1152/ajpcell.00125.2002

Yusuf, S., Hawken, S., Ounpuu, S., Dans, T., Avezum, A., Lanas, F., . . . Lisheng, L. (2004). Effect of potentially modifiable risk factors associated with myocardial infarction in 52 countries (the INTERHEART study): case-control study. *Lancet*, *364*(9438), 937-952. https://doi.org/10.1016/s0140-6736(04)17018-9

Zhang, H., Bajraszewski, N., Wu, E., Wang, H., Moseman, A. P., Dabora, S. L., . . . Kwiatkowski, D. J. (2007). PDGFRs are critical for PI3K/Akt activation and negatively regulated by mTOR. *The Journal of Clinical Investigation*, *117*(3), 730-738. https://doi.org/10.1172/JCI28984